A Unification of Models of Tethered Satellites

SIAM J. Applied Dynamical Systems
Vol. 10, No. 3, pp. 1042–1069

A Unification of Models of Tethered Satellites*

K. Uldall Kristiansen†, P. Palmer†, and M. Roberts†

Abstract. In this paper, different conservative models of tethered satellites are related mathematically, and it is established in what limit they may provide useful insight into the underlying dynamics. An infinite dimensional model is linked to a finite dimensional model, the slack-spring model, through a conjecture on the singular perturbation of tether thickness. The slack-spring model is then naturally related to a billiard model in the limit of an inextensible spring. Next, the motion of a dumbbell model, which is lowest in the hierarchy of models, is identified within the motion of the billiard model through a theorem on the existence of invariant curves by exploiting Moser's twist map theorem. Finally, numerical computations provide insight into the dynamics of the billiard model.

Key words. singular perturbed systems, mathematical modeling, tethered satellites, billiards

AMS subject classification. 37Nxx

DOI. 10.1137/090779887

1. Introduction.

Many applications have been proposed for spacecraft tether systems, ranging from the mundane to the highly speculative [4, 9]. The first tether was used in space in the late 1960s to stabilize attitude on the Gemini-12 spacecraft. More recently further tether experiments have been carried out to study the feasibility of long tethered systems in space. Examples include the SEDS-missions in 1993 and 1994 and the TiPS-mission launched in 1996 [9]. Cartmell and McKenzie survey current interest with their recent comprehensive review of space tether applications and experiments [9].

The tether literature presents a number of different tether models of varying complexity. The models can be divided into two groups: massive tether models and massless tether models. The massive tether models (see, e.g., [4, 16, 5]) couple a partial differential equation for the motion of the tether with two ordinary differential equations for the motions of the spacecraft. The spacecrafts are usually modeled as point masses. The massless tether models include the slack-spring model and the dumbbell model [4]. The slack-spring model is a finite dimensional model of tether dynamics wherein the tether is replaced by a spring connecting the satellites. The spring is assumed to go slack whenever the satellites are closer than the natural length of the tether. The dumbbell model, on the other hand, models the tethered system as a rigid rod. Clearly, such a model can capture only motion in which the tether is taut and is not adequate to describe the motion when the tether folds and bends. It is nonetheless widely used, for example, in the analysis of electrodynamical tether dynamics [26] and in three-body dynamics [12, 29].

*Received by the editors December 11, 2009; accepted for publication (in revised form) by T. Kaper May 3, 2011; published electronically September 20, 2011. This work was supported by EU funding for the Marie-Curie Research Training Network AstroNet (contract MRTN-CT-2006-035151).
http://www.siam.org/journals/siads/10-3/77988.html
†Surrey Space Centre and Department of Mathematics, University of Surrey, Guildford, GU2 7XH, UK (kristian.kristiansen@gmail.com, p.palmer@surrey.ac.uk, m.roberts@surrey.ac.uk).

Motivated by the slack-spring model, Beletsky and Pankova [6] suggested modeling inextensible tether dynamics as a billiards problem. They do not give any derivation of the model but do present a Poincaré mapping to study the dynamics. In another paper [30] the billiards model is used to study the dynamics of a viscoelastic tether and the transient chaotic oscillations of a tethered system. The viscoelasticity, or dissipation, due to the tether jerks, is taken into account by billiards restitution factors.

Aims of the paper. The different tether models described above have been studied and used in many references on orbiting tethered satellites. However, the relationships between them have never been explored in detail. In this paper we begin the task of unifying the models mathematically by showing how the simpler models can be derived rigorously from the more complicated models, and how solutions of the former perturb to solutions of the latter. We will mainly restrict our attention to the conservative models but will include discussions of dissipative versions at appropriate places.

In section 2 the different models are presented. In section 3 we show that the classical massive tether model is of mixed type, and it is argued that the model is ill-posed. We show that the inclusion of resistance to bending regularizes the problem so that the system admits a unique strong, local solution. We also show that noncollision and nonsingular parametrized solutions exist for all time. In section 4 we present a conjecture which states that in the limit of vanishing tether thickness, and for a *large* set of initial conditions, the solutions of the massive tether model converge to solutions of the slack-spring model. In section 5.2 a billiard model is then derived as the inextensible limit of the slack-spring model. This billiard model is then studied in section 6 using a Poincaré map. In the case that the center of mass of the system is moving on a circular orbit, we reduce this to a two dimensional symplectic map. The dumbbell dynamics is identified as embedded within the billiard dynamics, and KAM theory is used to show how it persists to the inextensible slack-spring model.

2. Tether models.

In this section several mathematical models of tether dynamics are presented. We consider two tethered satellites orbiting a spherical Earth; see Figure 1. The tether is modeled using linear elasticity, and we neglect nonconservative forces such as drag and viscoelasticity. Apart from the inclusion of bending resistance the equations obtained below are well known in the tether literature; see, e.g., [4].

2.1. Massive tether.

As indicated in Figure 1 the satellites are modeled as point masses positioned at $\mathbf{x}$ and $\mathbf{y}$ with masses $m_{\mathbf{x}}$ and $m_{\mathbf{y}}$, respectively. The tether is parametrized by

$$\mathbf{r} : [0,T] \times [0,l] \ni (t,s) \mapsto \mathbf{r}(t,s) \in \mathbb{R}^3,$$

l being the natural length of the tether. Letting ρ_l denote the line density, E Young's modulus, and A the cross-sectional area, we can derive the equations of the tethered system using a Lagrangian approach. Assuming linear elasticity the Lagrangian of the usual massive tether system considered in the literature is

$$L[\mathbf{w}, \partial_t \mathbf{w}] = K[\partial_t \mathbf{w}] - P[\mathbf{w}],$$

where

$$\mathbf{w} = (\mathbf{x}, \mathbf{y}, \mathbf{r}),$$

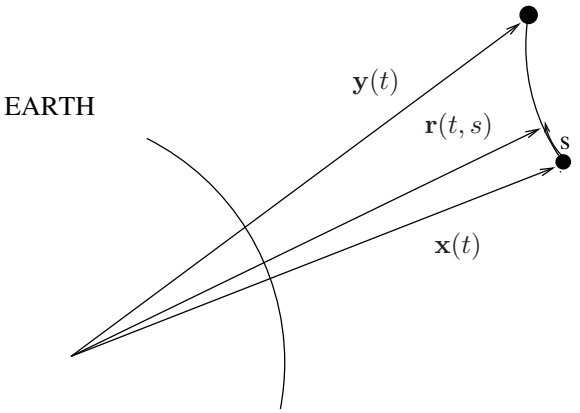

Figure 1. *A tethered satellite system.*

and K and P are the kinetic and the potential energies of the system:

$$K[\partial_t \mathbf{w}] = \frac{1}{2} m_{\mathbf{x}} |d_t \mathbf{x}|^2 + \frac{1}{2} m_{\mathbf{y}} |d_t \mathbf{y}|^2 + \frac{1}{2} \rho_l \int_0^l |\partial_t \mathbf{r}|^2 ds, \tag{1}$$

$$P[\mathbf{w}] = -\mu \frac{m_{\mathbf{x}}}{|\mathbf{x}|} - \mu \frac{m_{\mathbf{y}}}{|\mathbf{y}|} - \mu \rho_l \int_0^l |\mathbf{r}|^{-1} ds + \frac{EA}{2} \int_0^l \left(|\partial_s \mathbf{r}| - 1\right)^2 ds, \tag{2}$$

μ being the Earth's gravitational constant [17].[1,2,3] The last term on the right of (2) gives Hooke's law; see, e.g., [4]. We furthermore impose the boundary conditions

$$\mathbf{r}(t,0) = \mathbf{x}(t) \quad \text{and} \quad \mathbf{r}(t,l) = \mathbf{y}(t). \tag{3}$$

Hamilton's principle states that the solution, satisfying

$$\mathbf{w}|_{t=0} = \mathbf{w}_0 \quad \text{and} \quad \mathbf{w}|_{t=T} = \mathbf{w}_T, \tag{4}$$

is a critical path of the action S given by

$$S[\mathbf{w}] = \int_0^T L[\mathbf{w}, \partial_t \mathbf{w}] dt. \tag{5}$$

If $\mathbf{w}$ is classical, i.e., continuously differentiable with $\mathbf{r} \in C^{2,2}([0,T]\times[0,l])$, then by Hamilton's principle $\mathbf{w}$ satisfies the Euler–Lagrange equations

$$m_{\mathbf{x}} d_t^2 \mathbf{x} = -\mu \frac{m_{\mathbf{x}}}{|\mathbf{x}|^3} \mathbf{x} + EA \, \left(a_1(|\partial_s \mathbf{r}|)\partial_s \mathbf{r}\right)|_{s=0}, \tag{6}$$

$$m_{\mathbf{y}} d_t^2 \mathbf{y} = -\mu \frac{m_{\mathbf{y}}}{|\mathbf{y}|^3} \mathbf{y} - EA \, \left(a_1(|\partial_s \mathbf{r}|)\partial_s \mathbf{r}\right)|_{s=l}, \tag{7}$$

$$\rho_l \partial_t^2 \mathbf{r} = -\mu \frac{\rho_l}{|\mathbf{r}|^3} \mathbf{r} + EA \, \partial_s \left(a_1(|\partial_s \mathbf{r}|)\partial_s \mathbf{r}\right), \tag{8}$$

$$\mathbf{x} = \mathbf{r}|_{s=0}, \quad \mathbf{y} = \mathbf{r}|_{s=l}, \tag{9}$$

[1] We adapt the usual $[\cdot]$-notation to highlight that the input is a function.

[2] $d_t = \frac{d}{dt}$ and $\partial_x = \frac{\partial}{\partial x}$.

[3] $|\cdot|$ and $\|\cdot\|$ denote Euclidean norm and norms in infinite dimensional spaces, e.g., L^2 or Sobolev norms, respectively.

where a_1 is defined by

$$a_\zeta : \mathbb{R}\backslash\{0\} \ni x \mapsto a_\zeta(x) = \frac{x-\zeta}{x} \quad \text{for every} \quad \zeta > 0, \tag{10}$$

with $\zeta = 1$. The more general a_ζ, $\zeta > 0$, will later appear in the discussion and analysis of the slack-spring model. We shall discuss and analyze the assumption that $\mathbf{w}$ is classical in section 3.

As we shall argue later, the equations are ill-posed. To regularize them we add the term

$$B[\mathbf{r}] = \frac{EI}{2}\|\mathcal{K}[\mathbf{r}]\|^2$$

to $P[\mathbf{r}]$ to account for resistance against bending. Here I is the moment area of inertia, which for a circular cross-section is proportional to the fourth power of the diameter, and

$$\mathcal{K}[\mathbf{r}] = \frac{|\partial_s^2\mathbf{r} \times \partial_s\mathbf{r}|}{|\partial_s\mathbf{r}|^3}$$

is the geometrical curvature. Whenever $\mathbf{r}$ is unit-speed parametrized, $\mathcal{K}[\mathbf{r}] = |\partial_s^2\mathbf{r}|$ (see, e.g., [28, pp. 24–25], and a Taylor expansion in $|\partial_s\mathbf{r}|$ about 1 gives

$$\mathcal{K}[\mathbf{r}] = |\partial_s^2\mathbf{r}|\,(1 - 2\,(|\partial_s\mathbf{r}| - 1)) + \cdots .$$

Therefore, by virtue of the linear elasticity assumption $||\partial_s\mathbf{r}| - 1| \ll 1$, we arrive at the approximation

$$B[\mathbf{r}] \approx \frac{EI}{2}\|\partial_s^2\mathbf{r}\|^2.$$

From this approximation the inclusion of $\frac{EI}{2}\|\partial_s^2\mathbf{r}\|^2$ in the potential gives rise to a linear highest order differential operator in the Euler–Lagrange equations

$$m_{\mathbf{x}} d_t^2\mathbf{x} = -\mu\frac{m_{\mathbf{x}}}{|\mathbf{x}|^3}\mathbf{x} + EA\,(a_1(|\partial_s\mathbf{r}|)\partial_s\mathbf{r})\,|_{s=0} - EI\partial_s^3\mathbf{r}|_{s=0}, \tag{11}$$

$$m_{\mathbf{y}} d_t^2\mathbf{y} = -\mu\frac{m_{\mathbf{y}}}{|\mathbf{y}|^3}\mathbf{y} - EA\,(a_1(|\partial_s\mathbf{r}|)\partial_s\mathbf{r})\,|_{s=1} + EI\partial_s^3\mathbf{r}|_{s=l}, \tag{12}$$

$$\rho_l\partial_t^2\mathbf{r} = -\mu\frac{\rho_l}{|\mathbf{r}|^3}r + EA\,\partial_s\,(a_1(|\partial_s\mathbf{r}|)\partial_s\mathbf{r}) - EI\partial_s^4\mathbf{r}, \tag{13}$$

$$\mathbf{x} = \mathbf{r}|_{s=0}, \quad \mathbf{y} = \mathbf{r}|_{s=l},$$

now equipped with the natural boundary conditions

$$\partial_s^2\mathbf{r} = 0 \quad \text{for} \quad s = 0, 1. \tag{14}$$

The natural boundary conditions correspond to the inability of the tether to transfer bending to the hinged endpoints.

The equations (11), (12), (13) together with (3), (14) and initial conditions

$$\mathbf{w}(0) = \mathbf{w}_0, \quad \dot{\mathbf{w}}(0) = \dot{\mathbf{w}}_0$$

establish the *initial boundary value problem with dynamical boundaries*. We shall leave the introduction of appropriate sets of initial conditions to section 3. The relative equilibria of these models are not well studied, though a related problem is studied in [17].

To account for dissipation due to tether oscillations, the Kelvin–Voigt force [16, 4] can be added to the equations. This term is simply included by replacing a_1 by

$$\tilde{a}_1 = a_1 + \alpha|\partial_s r|^{-1}\partial_t|\partial_s r| = a_1 + \alpha\langle \partial_s r, \partial_{st}^2 r\rangle, \tag{15}$$

where $\alpha \geq 0$ is a dissipation constant.

2.2. Massless tethers and the slack-spring model. In the slack-spring model the tether inertia is neglected and the tether only affects the motion when it is taut and the distance between the satellites is greater than the natural length l. The direction of the tether force is directed along the relative position vector as an ideal spring with stiffness $k = \frac{EA}{l}$. The equations are

$$m_{\mathbf{x}} d_t^2 \mathbf{x} = -\mu \frac{m_{\mathbf{x}}}{|\mathbf{x}|^3}\mathbf{x} + k\,\widehat{a}_l(|\mathbf{y}-\mathbf{x}|)(\mathbf{y}-\mathbf{x}), \tag{16}$$

$$m_{\mathbf{y}} d_t^2 \mathbf{y} = -\mu \frac{m_{\mathbf{x}}}{|\mathbf{y}|^3}\mathbf{y} + k\,\widehat{a}_l(|\mathbf{y}-\mathbf{x}|)(\mathbf{x}-\mathbf{y}), \tag{17}$$

where

$$\widehat{a}_l(p) = \mathbf{1}_{\{p-l>0\}} a_l(p) \quad \text{for every} \quad p \geq 0, \tag{18}$$

and $\mathbf{1}_{\{p-l>0\}}$ is the Heaviside function.

Let $M = m_{\mathbf{x}} + m_{\mathbf{y}}$ be the total mass and $\mu_{\mathbf{x}} = \frac{m_{\mathbf{x}}}{M}$ and $\mu_{\mathbf{y}} = \frac{m_{\mathbf{y}}}{M} = 1 - \mu_{\mathbf{x}}$ the mass ratios. Writing the Lagrangian in terms of the center of mass and relative position coordinates

$$\begin{aligned} \mathbf{q} &= \mu_{\mathbf{y}}\mathbf{y} + \mu_{\mathbf{x}}\mathbf{x}, \\ \boldsymbol{\delta}\mathbf{q} &= \mathbf{y} - \mathbf{x} \end{aligned}$$

(see Figure 2) and applying the Legendre transformation, we end up with the Hamiltonian

$$\begin{aligned} H_{\mathrm{ST}}(\mathbf{q}, \boldsymbol{\delta}\mathbf{q}, \mathbf{p}, \boldsymbol{\delta}\mathbf{p}) = \frac{1}{2\xi}|\mathbf{p}|^2 + \frac{1}{2}|\boldsymbol{\delta}\mathbf{p}|^2 - \frac{1}{\mu_{\mathbf{x}}}\frac{\mu}{|\mathbf{q} + \mu_{\mathbf{x}}\boldsymbol{\delta}\mathbf{q}|} - \frac{1}{\mu_{\mathbf{y}}}\frac{\mu}{|\mathbf{q} - \mu_{\mathbf{y}}\boldsymbol{\delta}\mathbf{q}|} \\ + \kappa \mathbf{1}_{|\boldsymbol{\delta}\mathbf{q}|-l}\left(|\boldsymbol{\delta}\mathbf{q}| - l\right)^2, \end{aligned} \tag{19}$$

endowed with the symplectic form

$$\omega = d\mathbf{q} \wedge d\mathbf{p} + d\boldsymbol{\delta}\mathbf{q} \wedge d\boldsymbol{\delta}\mathbf{p}.$$

Here $\xi = 1/(\mu_{\mathbf{x}}\mu_{\mathbf{y}})$ and $\kappa = k\, m_{\mathbf{y}} m_{\mathbf{x}}/2M$.

The Hamiltonian is SO(3)-invariant and therefore conserves angular momentum:

$$\mathbf{J} = \mathbf{q} \wedge \mathbf{p} + \boldsymbol{\delta}\mathbf{q} \wedge \boldsymbol{\delta}\mathbf{p}.$$

Relative equilibria of the slack-spring system are critical points of the Hamiltonian restricted to the level sets of the momentum map. To study the planar equilibria it is beneficial to

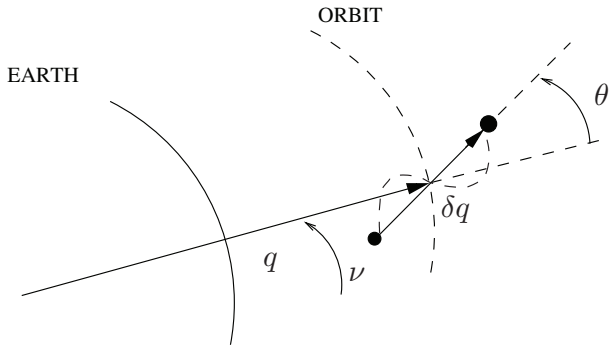

Figure 2. *Tethered satellite system: The slack-spring approximation.*

introduce the true anomaly ν and the shape coordinate θ, which is invariant under the action of S^1, together with the two radii r and δr; see Figure 2. In particular, we apply the following symplectomorphism to symplectic polar coordinates:

$$\mathbf{q} = r\begin{pmatrix}\cos\nu\\ \sin\nu\end{pmatrix}, \quad \boldsymbol{\delta}\mathbf{q} = \delta r\begin{pmatrix}\cos(\nu+\theta)\\ \sin(\nu+\theta)\end{pmatrix},$$
$$p_\nu = r\mathbf{p}\cdot(-\sin\nu,\cos\nu) + \delta r\boldsymbol{\delta}\mathbf{p}\cdot(-\sin(\nu+\theta),\cos(\nu+\theta)),$$
$$p_\theta = \delta r\boldsymbol{\delta}\mathbf{p}\cdot(-\sin(\nu+\theta),\cos(\nu+\theta)),$$
$$p_r = \mathbf{p}\cdot(\cos\nu,\sin\nu), \quad p_{\delta r} = \boldsymbol{\delta}\mathbf{p}\cdot(\cos(\nu+\theta),\sin(\nu+\theta)).$$

Then ν becomes cyclic in the Hamiltonian,

$$\begin{aligned} H_{\mathrm{ST}}(r,\delta r,\nu,\theta,p_r,p_{\delta r},p_\nu,p_\theta) = {} & \frac{1}{2\xi}p_r^2 + \frac{1}{2}p_{\delta r}^2 + \frac{1}{2\xi r^2}(p_\nu - p_\theta)^2 + \frac{1}{2\delta r^2}p_\theta^2 \\ & - \frac{1}{\mu_{\mathbf{x}}}\frac{\mu}{\sqrt{r^2+\mu_{\mathbf{x}}^2\delta r^2 + 2\mu_{\mathbf{x}} r\delta r\cos\theta}} \\ & - \frac{1}{\mu_{\mathbf{y}}}\frac{\mu}{\sqrt{r^2+\mu_{\mathbf{y}}^2\delta r^2 - 2\mu_{\mathbf{y}} r\delta r\cos\theta}} \\ & + \kappa\mathbf{1}_{\delta r - l}\,(\delta r - l)^2\,, \end{aligned} \tag{20}$$

and $J = p_\nu \in \mathbb{R}$. The study of relative equilibria and their stability becomes a straightforward, though tedious, computation. This shows that there exist two different types of relative equilibria: the tether can be either tangent or normal to the circular orbit on which the center of mass moves; see Figure 3. Due to the inability of the slack-spring to be in compression there do not exist any relative equilibria where the relative position between the satellites $\boldsymbol{\delta}\mathbf{q}$ is perpendicular to the plane in which the center of mass moves. Upon introducing elevation coordinates z and δz to the direction of $\mathbf{J} = (0,0,p_\nu)$, the energy-momentum method [23] can, for realistic tether lengths, $l \ll r$, be used to show that the relative equilibria with $z = \delta z = 0$ for which the system is aligned normal to a circular orbit are orbitally stable. On the other hand, the tangential relative equilibria are unstable. For more details on the stability and bifurcations when $l = \mathcal{O}(r)$, see [19, 7].

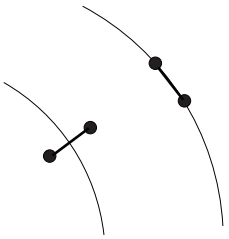

Figure 3. *Relative equilibria of the slack-spring model.*

To account for dissipation in the slack-spring model we can replace a_l by $\tilde{a}_l = a_l + \alpha|\boldsymbol{\delta}\mathbf{q}|^{-1}d_t|\boldsymbol{\delta}\mathbf{q}|$. This is a slack-spring version of the Kelvin–Voigt model. This assumes that the system does not dissipate energy when the spring is slack. Let us consider the effect of this dissipation on an orbitally stable relative equilibrium where the system is normal to the circular orbiting center of mass. Then the tether is stretched $\delta r > l$. We may therefore consider a neighborhood of the equilibrium in which $\delta r > l$. Then in the coordinates introduced above, the equations of motion with dissipation therefore coincide with Hamilton's equations except for the equation for $p_{\delta r}$, which now reads

$$\dot{p}_{\delta r} = -\partial_{\delta r} H_{\mathrm{ST}} - 2\kappa\alpha p_{\delta r}.$$

It follows that $\dot{H}_{\mathrm{ST}} = -\kappa\alpha p_{\delta r}^2 \leq 0$. Furthermore, if $p_{\delta r} \equiv 0$, then the system is in a relative equilibrium. Therefore, H_{ST} is a strict Lyapunov function so that the relative equilibrium perturbs to an asymptotically stable relative equilibrium.

2.3. The dumbbell model. In the dumbbell model the tether is replaced by a rigid rod. The system is again Hamiltonian, now on T^*Q, where $Q = (\mathbb{R}^3 \times S_l^2)\backslash\mathcal{C}$, $S_l^2 = \{\mathbf{q} \in \mathbb{R}^3 | |\mathbf{q}| = l\}$, $\mathcal{C}$ being the closed collision set. The symplectic polar coordinates introduced above for the slack-spring model are, upon fixing $\delta r = l$, also appropriate in the study of relative equilibria of the dumbbell dynamics; cf. [18, 19]. There exist three relative equilibria: tangent and normal to the circular orbiting center of mass, as seen in Figure 3, and, finally, an equilibrium for which the dumbbell attitude is normal to the plane defined by the SO(3)-orbit. The dumbbell model therefore has an additional relative equilibrium compared to the slack-spring model. A comprehensive stability analysis is provided in [18, 19].

3. Well-posedness of the massive tether models. In section 2.1 it was assumed that the critical point of the action, (5), was classical. More often than not, to establish existence in variational problems and partial differential equations it is necessary to enlarge the set of the admissible functions. With a bit of extra care, the derivation of the Euler–Lagrange equations can be extended to these enlarged spaces.

In the following we shall investigate the well-posedness of the tether modeling including and neglecting the resistance against bending, $EI \neq 0$, respectively, $EI = 0$. Despite the complete neglect of this term in the engineering literature, we shall see that, at least from a mathematically point of view, its inclusion is essential.

3.1. $EI \neq 0$. For simplicity we set all constants to 1 and introduce $\mathbf{u} = \mathbf{r} - s\mathbf{y} - (1-s)\mathbf{x}$ so the boundary conditions become homogeneous. Let $\mathbf{f}(\mathbf{z}) = -\mathbf{z}|\mathbf{z}|^{-3}$, $\mathbf{z} \in \mathbb{R}^3\backslash\{0\}$. The

equations (11), (12), and (13) then take the form

$$\partial_t^2 \mathbf{u} = -\partial_s^4 \mathbf{u} + \partial_s \left(a_1(|\partial_s \mathbf{r}|)\partial_s \mathbf{r}\right) + \mathbf{h}(\mathbf{u}, \mathbf{x}, \mathbf{y})(s), \tag{21}$$

$$d_t^2 \mathbf{x} = \mathbf{f}(\mathbf{x}) + a_1(|\partial_s \mathbf{r}|)\partial_s \mathbf{r}|_{s=0} - \partial_s^3 \mathbf{u}|_{s=0}, \tag{22}$$

$$d_t^2 \mathbf{y} = \mathbf{f}(\mathbf{y}) - a_1(|\partial_s \mathbf{r}|)\partial_s \mathbf{r}|_{s=1} + \partial_s^3 \mathbf{u}|_{s=1}, \tag{23}$$

$$\mathbf{u} = 0 = \partial_s^2 \mathbf{u} \quad \text{for} \quad s = 0, 1,$$

with

$$\begin{aligned} \mathbf{h}(\mathbf{u}, \mathbf{x}, \mathbf{y})(s) &= \mathbf{f}(\mathbf{r}) - \left(s d_t^2 \mathbf{y} + (1-s) d_t^2 \mathbf{x}\right) \\ &= \mathbf{f}(\mathbf{r}) - s\left(\mathbf{f}(\mathbf{y}) - a_1(|\partial_s \mathbf{r}|)\partial_s \mathbf{r}|_{s=1} + \partial_s^3 \mathbf{u}|_{s=1}\right) \\ &\quad - (1-s)\left(\mathbf{f}(\mathbf{x}) + a_1(|\partial_s \mathbf{r}|)\partial_s \mathbf{r}|_{s=0} - \partial_s^3 \mathbf{u}|_{s=0}\right), \end{aligned} \tag{24}$$

together with a set of initial conditions

$$\begin{aligned} \mathbf{u}|_{t=0} = \mathbf{u}_0 \in U, \quad \partial_t \mathbf{u}|_{t=0} = \dot{\mathbf{u}}_0 \in V, \\ \mathbf{x}(0) = \mathbf{x}_0 \in \mathbb{R}^3 \backslash \{0\}, \quad \dot{\mathbf{x}}(0) = \dot{\mathbf{x}}_0 \in \mathbb{R}^3, \\ \mathbf{y}(0) = \mathbf{y}_0 \in \mathbb{R}^3 \backslash \{0\}, \quad \dot{\mathbf{y}}(0) = \dot{\mathbf{y}}_0 \in \mathbb{R}^3. \end{aligned} \tag{25}$$

Here we have introduced the spaces

$$\begin{aligned} U &= \{\mathbf{u} \in W^4((0,1); \mathbb{R}^3) |\, \mathbf{u} = 0 = \partial_s^2 \mathbf{u} \text{ for } s = 0, 1\}, \\ V &= W^2((0,1); \mathbb{R}^3) \cap W_0^1((0,1); \mathbb{R}^3). \end{aligned}$$

Here W^n is the nth Sobolev space. In particular, W_0^n is the completion of C_0^∞ in the W^n-norm whose elements' first $n-1$ (weak) derivatives all leave *zero trace* on the boundary [25, Theorem 9.16, p. 123]. For a comprehensive and very rigorous introduction to Sobolev spaces see [1, 13]. For a less formal description see [11]. We equip $U \times V$ with a $W^4 \times W^2$-type norm:

$$\|(\mathbf{u}, \mathbf{v})\|_{U \times V}^2 = \|\partial_s^2 \mathbf{v}\|_{L^2((0,1);\mathbb{R}^3)}^2 + \|\partial_s^4 \mathbf{u}\|_{L^2((0,1);\mathbb{R}^3)}^2.$$

That this defines a norm on $U \times V$ follows from Poincaré's inequality [11]. Let

$$\begin{aligned} \mathcal{S}_\tau = C_{L^\infty}^2([0,\tau); \mathbb{R}^3) \times C_{L^\infty}^0([0,\tau); U) \times C_{L^\infty}^2([0,\tau); \mathbb{R}^3) \\ \times C_{L^\infty}^1([0,\tau); \mathbb{R}^3) \times C_{L^\infty}^0([0,\tau); V) \times C_{L^\infty}^1([0,\tau); \mathbb{R}^3) \end{aligned} \tag{26}$$

and

$$\mathcal{X} = \{(\mathbf{x}_0, \mathbf{u}_0, \mathbf{y}_0, \dot{\mathbf{x}}_0, \mathbf{v}_0, \dot{\mathbf{y}}_0) |\, |\mathbf{x}_0|,\ |\mathbf{y}_0|,\ |\mathbf{r}_0| > 0,\ |\partial_s \mathbf{r}_0| > 0,\ \mathbf{u}_0 \in U,\ \mathbf{v}_0 \in V\}, \tag{27}$$

where $\mathbf{r}_0 = \mathbf{u}_0 + s\mathbf{y}_0 + (1-s)\mathbf{x}_0$. Local existence, uniqueness, and continuous dependence on initial conditions may then be proved.

Theorem 1. *The system of* (21), (22), *and* (23) *with initial conditions* (25) *admits a unique strong solution in* $\mathcal{S}_T$ (26), *for some* $T = T(\boldsymbol{w}_0) > 0$, *that depends continuously on the initial conditions* $\boldsymbol{w}_0 \in \mathcal{X}$ (27), *within its interval of existence. If the solution satisfies*

$$|\partial_s \boldsymbol{r}|,\ |\boldsymbol{r}| \geq \delta, \tag{28}$$

for some $\delta > 0$, *then the solution exists globally so that* $T = \infty$. *Finally, the solution preserves energy.*

Proof. The techniques involved are standard (see, e.g., [32, 31]), and we therefore aim only to give a proof of the existence. The uniqueness, continuous dependence on initial conditions and energy preservation will follow from estimates similar to those obtained below.

We will assume that (28) holds true for some (small) $\delta > 0$ and that it holds true with strict inequality at $t = 0$. In the following let C_i, $i \in \mathbb{N}$, be constants that depend only upon initial conditions and δ. We will prove the existence by a Galerkin approximation. For this we will need to obtain a priori estimates. First, we note that from the energy conservation it follows by (28) that

$$\|\partial_s^2 \mathbf{u}\|_{L^2} \leq C_1. \tag{29}$$

Next, we shall then show that this allows us to obtain a higher order a priori estimate of $(\mathbf{u}, \partial_t \mathbf{u})$ in $L^\infty([0,T]; U \times V)$. Here $T > 0$ is some fixed constant. Upon dotting the equation for $\mathbf{r}$ by $\partial_t \partial_s^4 \mathbf{u}$ and integrating by parts, we arrive at[4]

$$\begin{aligned}\frac{1}{2}\partial_t \|\partial_s^2 \mathbf{v}\|_{L^2}^2 + \frac{1}{2}\partial_t \|\partial_s^4 \mathbf{u}\|_{L^2}^2 + \langle d_t^2 \mathbf{y} - \mathbf{f}(\mathbf{y}), \partial_t \partial_s^3 \mathbf{u}|_{s=1}\rangle - \langle d_t^2 \mathbf{x} - \mathbf{f}(\mathbf{x}), \partial_t \partial_s^3 \mathbf{u}|_{s=0}\rangle \\ = \langle\langle \partial_s^3 (a_1(|\partial_s \mathbf{r}|)\partial_s \mathbf{r}), \partial_t \partial_s^2 \mathbf{u}\rangle\rangle + \langle\langle \partial_s^2 \mathbf{f}(\mathbf{r}), \partial_t \partial_s^2 \mathbf{u}\rangle\rangle,\end{aligned}$$

where $\langle \cdot, \cdot \rangle$ and $\langle\langle \cdot, \cdot \rangle\rangle$ are the Euclidean and $L^2((0,1); \mathbb{R}^3)$ inner products, respectively, or simply by (22) and (23)

$$\begin{aligned}\frac{1}{2}\partial_t \|\partial_s^2 \mathbf{v}\|_{L^2}^2 + \frac{1}{2}\partial_t \|\partial_s^4 \mathbf{u}\|_{L^2}^2 + \frac{1}{2}\partial_t |d_t^2 \mathbf{y} - \mathbf{f}(\mathbf{y})|^2 + \frac{1}{2}\partial_t |d_t^2 \mathbf{x} - \mathbf{f}(\mathbf{x})|^2 \\ = \langle\langle \partial_s^3 (a_1(|\partial_s \mathbf{r}|)\partial_s \mathbf{r}), \partial_t \partial_s^2 \mathbf{u}\rangle\rangle + \langle\langle \partial_s^2 \mathbf{f}(\mathbf{r}), \partial_t \partial_s^2 \mathbf{u}\rangle\rangle \\ + \langle d_t^2 \mathbf{y} - \mathbf{f}(\mathbf{y}), \partial_t (a_1(|\partial_s \mathbf{r}|)\partial_s \mathbf{r})|_{s=1}\rangle + \langle d_t^2 \mathbf{x} - \mathbf{f}(\mathbf{x}), \partial_t (a_1(|\partial_s \mathbf{r}|)\partial_s \mathbf{r})|_{s=0}\rangle.\end{aligned} \tag{30}$$

The equations (22) and (23) also give

$$\begin{aligned}\frac{1}{2} d_t |\mathbf{x}|^2 + \frac{1}{2} d_t |\dot{\mathbf{x}}|^2 &= \langle \mathbf{x}, d_t \mathbf{x}\rangle + \langle \mathbf{f}(\mathbf{x}), d_t \mathbf{x}\rangle + \langle a_1(|\partial_s \mathbf{r}|)\partial_s \mathbf{r}|_{s=0} - \partial_s^3 \mathbf{u}|_{s=0}, d_t \mathbf{x}\rangle, \\ \frac{1}{2} d_t |\mathbf{y}|^2 + \frac{1}{2} d_t |\dot{\mathbf{y}}|^2 &= \langle \mathbf{y}, d_t \mathbf{y}\rangle + \langle \mathbf{f}(\mathbf{y}), d_t \mathbf{y}\rangle + \langle -a_1(|\partial_s \mathbf{r}|)\partial_s \mathbf{r}|_{s=1} + \partial_s^3 \mathbf{u}|_{s=1}, d_t \mathbf{y}\rangle,\end{aligned}$$

which together with (30) upon consecutive applications of standard functional analytic inequalities guarantees the existence of C_{10} and C_{11} such that

$$\begin{aligned}\frac{1}{2}\partial_t \Big(&\|\partial_s^2 \mathbf{v}\|_{L^2}^2 + \|\partial_s^4 \mathbf{u}\|_{L^2}^2 + |\mathbf{x}|^2 + |d_t \mathbf{x}|^2 + |\mathbf{y}|^2 + |d_t \mathbf{y}|^2 \\ &+ |d_t^2 \mathbf{x} - \mathbf{f}(\mathbf{x})|^2 + |d_t^2 \mathbf{y} - \mathbf{f}(\mathbf{y})|^2 \Big) \\ \leq C_{10} + C_{11} \Big(&\|\partial_s^2 \mathbf{v}\|_{L^2}^2 + \|\partial_s^4 \mathbf{u}\|_{L^2}^2 + |\mathbf{x}|^2 + |d_t \mathbf{x}|^2 + |\mathbf{y}|^2 + |d_t \mathbf{y}|^2 \\ &+ |d_t^2 \mathbf{x} - \mathbf{f}(\mathbf{x})|^2 + |d_t^2 \mathbf{y} - \mathbf{f}(\mathbf{y})|^2 \Big).\end{aligned} \tag{31}$$

[4] Strictly upon extension by continuity.

The main difficulty here is to obtain the required control of the term

$$\langle\langle \partial_s^3(a_1(|\partial_s \mathbf{r}|)\partial_s \mathbf{r}), \partial_t \partial_s^2 \mathbf{u}\rangle\rangle.$$

However, by (28) and (29) it follows upon applying the Hölder inequality that

$$\begin{aligned} |\partial_s^3(a_1(|\partial_s \mathbf{r}|)\partial_s \mathbf{r})| &\le C_2|\partial_s^2 \mathbf{r}|^3 + C_3|\partial_s^2 \mathbf{r}||\partial_s^3 \mathbf{r}| + C_4|\partial_s^4 \mathbf{r}| \\ &= C_2|\partial_s^2 \mathbf{u}|^3 + C_3|\partial_s^2 \mathbf{r}||\partial_s^3 \mathbf{u}| + C_4|\partial_s^4 \mathbf{u}|, \end{aligned} \tag{32}$$

and therefore

$$\begin{aligned} \langle\langle \partial_s^3(a_1(|\partial_s \mathbf{r}|)\partial_s \mathbf{r}), \partial_t \partial_s^2 \mathbf{u}\rangle\rangle &\le (\text{using the Cauchy–Schwarz inequality in } \mathbb{R}^3) \\ &\le \| |\partial_s^3(a_1(|\partial_s \mathbf{r}|)\partial_s \mathbf{r})||\partial_t \partial_s^2 \mathbf{u}| \|_{L^1} \\ &\le (\text{using (32) and Young's inequality}) \\ &\le \frac{1}{2}C_2^2 \|\partial_s^2 \mathbf{u}\|_{L^6}^6 + \frac{1}{2}C_3^2 \| |\partial_s^2 \mathbf{u}||\partial_s^3 \mathbf{u}| \|_{L^2}^2 + \frac{1}{2}C_4^2 \|\partial_s^4 \mathbf{u}\|_{L^2}^2 \\ &\quad + \frac{1}{2}(C_2^2 + C_3^2 + C_4^2)\|\partial_t \partial_s^2 \mathbf{u}\|\|_{L^2}^2. \end{aligned}$$

To estimate the first term on the right-hand side of this inequality we use the Gagliardo–Nirenberg inequality [22] to interpolate L^6 between L^2 and $W^2 \cap W_0^1$:

$$\|\partial_s^2 \mathbf{u}\|_{L^6}^6 \le C_5 \|\partial_s^2 \mathbf{u}\|_{L^2}^5 \|\partial_s^4 \mathbf{u}\|_{L^2} \le (\text{using (29)}) \le C_5 C_1^5 \|\partial_s^4 \mathbf{u}\|_{L^2}.$$

For the second term we use the embedding $W^4 \hookrightarrow C_{L^\infty}^3$:

$$\| |\partial_s^2 \mathbf{u}||\partial_s^3 \mathbf{u}| \|_{L^2}^2 \le \|\partial_s^2 \mathbf{u}\|_{L^2}^2 \|\partial_s^3 \mathbf{u}\|_{L^\infty}^2 \le (\text{using (29)}) \le C_1^2 \|\partial_s^3 \mathbf{u}\|_{L^\infty}^2 \le C_6 C_1^2 \|\partial_s^4 \mathbf{u}\|_{L^2}^2.$$

It therefore follows that

$$\langle\langle \partial_s^3(a_1(|\partial_s \mathbf{r}|)\partial_s \mathbf{r}), \partial_t \partial_s^2 \mathbf{u}\rangle\rangle \le C_7 + C_8 \|\partial_s^4 \mathbf{u}\|_{L^2}^2 + C_9 \|\partial_s^2 \partial_t \mathbf{u}\|_{L^2}^2.$$

Through Gronwall's inequality, (31) gives

$$\begin{aligned} &\Big(\|\partial_s^2 \mathbf{v}\|_{L^2}^2 + \|\partial_s^4 \mathbf{u}\|_{L^2}^2 + |\mathbf{x}|^2 + |d_t \mathbf{x}|^2 + |\mathbf{y}|^2 + |d_t \mathbf{y}|^2 \\ &\quad + |d_t^2 \mathbf{x} - \mathbf{f}(\mathbf{x})|^2 + |d_t^2 \mathbf{y} - \mathbf{f}(\mathbf{y})|^2 \Big) \\ &\le \Big(2C_{10} t + \Big(\|\partial_s^2 \mathbf{v}\|_{L^2}^2 + \|\partial_s^4 \mathbf{u}\|_{L^2}^2 + |\mathbf{x}|^2 + |d_t \mathbf{x}|^2 + |\mathbf{y}|^2 + |d_t \mathbf{y}|^2 \\ &\qquad + |d_t^2 \mathbf{x} - \mathbf{f}(\mathbf{x})|^2 + |d_t^2 \mathbf{y} - \mathbf{f}(\mathbf{y})|^2 \Big)|_{t=0} \Big) \exp(2C_{11} t), \quad t \in [0, T). \end{aligned}$$

Finally, from (21) it follows that $\partial_t^2 \mathbf{u} \in L^\infty([0,T]; L^2)$.

We are now ready to prove the existence of the solution. To do so we let $\{\mathbf{e}_i\}_{i=1}^\infty$ be the orthonormal basis in L^2 generated by the eigenvectors of the self-adjoint operator ∂_s^4 defined

on the space U. Furthermore, we let Π_N be the orthoprojector to the first N eigenvectors in L^2, $L^2_N = \Pi_N L^2$. We write $\mathbf{u}_N = \Pi_N \mathbf{u}$ and $\mathbf{r}_N = \mathbf{u}_N + (1-s)\mathbf{x} + s\mathbf{y}$ and consider the approximation

$$\partial_t^2 \Pi_N \mathbf{r}_N = -\partial_s^4 \mathbf{r}_N + \Pi_N \partial_s \left(a_1(|\partial_s \mathbf{r}_N|)\partial_s \mathbf{r}_N\right) + \Pi_N \mathbf{f}(\mathbf{r}_N), \tag{33}$$

$$d_t^2 \mathbf{x} = \mathbf{f}(\mathbf{x}) + a_1(|\partial_s \mathbf{r}_N|)\partial_s \mathbf{r}_N|_{s=0} - \partial_s^3 \mathbf{u}_N|_{s=0}, \tag{34}$$

$$d_t^2 \mathbf{y} = \mathbf{f}(\mathbf{y}) - a_1(|\partial_s \mathbf{r}_N|)\partial_s \mathbf{r}_N|_{s=1} + \partial_s^3 \mathbf{u}_N|_{s=1}. \tag{35}$$

This is now a finite dimensional system with smooth right-hand side, and the existence of the solution of the approximation therefore follows. We recall the property

$$\langle\langle \Pi_N \mathbf{F}, \mathbf{v}_N \rangle\rangle = \langle\langle \mathbf{F}, \mathbf{v}_N \rangle\rangle \tag{36}$$

for every $\mathbf{v}_N \in L^2_N$ and $\mathbf{F} \in L^2$. Furthermore, if $\mathbf{z}_N = \mathbf{v}_N + f(s)\mathbf{w}$, $\mathbf{v}_N \in L^2_N$, $\mathbf{w} \in \mathbb{R}^3$, and $f \in L^2((0,1);\mathbb{R})$, then

$$\begin{aligned}\langle\langle \Pi_N \mathbf{F}, \mathbf{z}_N \rangle\rangle &= \langle\langle \mathbf{F}, \Pi_N \mathbf{z}_N \rangle\rangle \\ &= \langle\langle \mathbf{F}, \mathbf{z}_N - \mathbf{w}\Pi_N^\perp f(s) \rangle\rangle \\ &= \langle\langle \mathbf{F}, \mathbf{z}_N \rangle\rangle - \langle\langle \mathbf{F}, \mathbf{w}\Pi_N^\perp f(s) \rangle\rangle,\end{aligned}$$

and

$$\begin{aligned}&\langle\langle \mathbf{F}, \mathbf{w}\Pi_N^\perp f(s) \rangle\rangle \le \|\mathbf{F}\|_{L^2} |w| \|\Pi_N^\perp f(s)\|_{L^2} \\ &\le \frac{1}{2}\|\Pi_N^\perp f(s)\|_{L^2} \left(\|\mathbf{F}\|_{L^2}^2 + |w|^2\right).\end{aligned}$$

Here the right-hand side approaches 0 uniformly for $N \to \infty$. The estimates above can then with little effort be repeated to conclude that

$$\|\partial_t \partial_s^2 \mathbf{u}_N\|_{L^2},\ \|\partial_s^4 \mathbf{u}_N\|_{L^2},\ \|\partial_t^2 \mathbf{u}_N\|_{L^2} \le C,$$

with C independent of N. In fact (31) extends identically due to (36). We can then pass to the limit $N \to \infty$ to conclude weak-* convergence to a $\boldsymbol{\xi} = (\mathbf{u}, \partial_t \mathbf{u})$ in $L^\infty([0,T]; U \times V) \cap \{\partial_t^2 \mathbf{u} \in L^\infty([0,T]; L^2)\}$. However, by the compactness of the embedding

$$L^\infty([0,T]; U \times V) \cap \{\partial_t^2 \mathbf{u} \in L^\infty([0,T]; L^2)\} \subset C^0_{L^\infty}([0,T]; V \times L^2)$$

(see, e.g., [31]), we may actually conclude strong converge to $\boldsymbol{\xi}$ in $C^0_{L^\infty}([0,T]; V \times L^2)$. To show that this limit solves the equation, we have to pass to the limit in the nonlinear term:

$$\partial_s \left(a_1(|\partial_s \mathbf{r}_N|)\partial_s \mathbf{r}_N\right) = \mathbf{M}(\partial_s \mathbf{r}_N)\partial_s^2 \mathbf{u}_N \to \mathbf{M}(\partial_s \mathbf{r})\partial_s^2 \mathbf{u}, \tag{37}$$

where

$$\mathbf{M}(\mathbf{p}) = a_1(|\mathbf{p}|)\mathbf{I} + \frac{\mathbf{p}\mathbf{p}^T}{|\mathbf{p}|^3} \in \mathbb{R}^{3\times 3}, \quad \mathbf{p} \in \mathbb{R}^3. \tag{38}$$

To do so we first recall that $W^2((0,1);\mathbb{R}^3) \subset C^1_{L^\infty}([0,1];\mathbb{R}^3)$ and therefore $\mathbf{M}_N \to \mathbf{M}$ by (28) in $C^0_{L^\infty}([0,1];\mathbb{R}^3)$. We write $\mathbf{M}_N = \mathbf{M} + \boldsymbol{\epsilon}_N$ with $\boldsymbol{\epsilon}_N \to 0$ in $C^0_{L^\infty}([0,1];\mathbb{R}^3)$ so that

$$\|\mathbf{M}_N \partial_s^2 \mathbf{u}_N - \mathbf{M}\partial_s^2 \mathbf{u}\|_{L^2} \leq \|\mathbf{M}\left(\partial_s^2 \mathbf{u}_N - \partial_s^2 \mathbf{u}\right)\|_{L^2} + \|\boldsymbol{\epsilon}_N\|_{L^2} \|\partial_s^2 \mathbf{u}_N\|_{L^2} \to 0$$

for $N \to \infty$. Therefore, it has been shown that $\mathbf{M}_N \partial_s^2 \mathbf{u}_N \to \mathbf{M}\partial_s^2 \mathbf{u}$ in L^2 and $\boldsymbol{\xi}$ is therefore a solution. By repeating the arguments in [32] it can actually be established that $\boldsymbol{\xi} \in C^0_{L^\infty}([0,T];U \times V)$.

Now, recall that (28) was assumed to hold true with strict inequality at $t = 0$. Then by the continuity of $\mathbf{r}$ and $\partial_s \mathbf{r}$ it follows that (28) still holds true for T sufficiently small. This completes the proof of the local existence and also the global existence when the singularities are not encountered. ∎

3.2. Well-posedness with Kelvin–Voigt dissipation. The addition of the dissipative Kelvin–Voigt term (replacing a_1 by $\tilde{a}_1$ (15)) complicates this analysis. The Galerkin method relies on an a priori $U \times V$-estimate similar to the one established above. Upon multiplying the equations by $\partial_t \partial_s^4 u^T$ and integrating by parts we end up with (30) but with a_1 replaced by $\tilde{a}_1$ (15). However, the term $\langle\langle \partial_s^3(\tilde{a}_1(|\partial_s \mathbf{r}|)\partial_s \mathbf{r}), \partial_t \partial_s^2 \mathbf{u}\rangle\rangle$ cannot be controlled in $U \times V$ as a term including $\partial_s^4 \mathbf{v}$ appears. We need $U \times V$-estimates to control the traces appearing in the boundary equations (22) and (23). There is a lack of two derivatives. These issues could certainly be circumvented by the addition of a term $\partial_t \partial_s^4 \mathbf{r}$ due to bending dissipation. As we have mainly restricted our attention to conservative models, this shall not be pursued further in this research.

3.3. $EI = 0$. For simplicity we set $\mu = 0$ and all other constants to 1. The equations (6), (7), and (8) then become

$$\begin{aligned} d_t^2 \mathbf{x} &= (a_1(|\mathbf{r}|)\partial_s \mathbf{r})\,|_{s=0}, \\ d_t^2 \mathbf{y} &= -(a_1(|\mathbf{r}|)\partial_s \mathbf{r})\,|_{s=1}, \\ \partial_t^2 \mathbf{r} &= \partial_s\left(a_1(|\partial_s \mathbf{r}|)\partial_s \mathbf{r}\right), \\ \mathbf{x} &= \mathbf{r}|_{s=0}, \quad \mathbf{y} = \mathbf{r}|_{s=1}. \end{aligned}$$

In the following we demonstrate that in this case the hope of obtaining existence of a strong solution is futile. The problem is quasi-linear, which follows from the computation in (37). The matrix $\mathbf{M}(\mathbf{p})$ (38) is symmetric, and it is therefore diagonalizable for every $\mathbf{p} \neq 0$ with real eigenvalues and orthogonal eigenspaces. We furthermore notice that $\mathbf{b}(\mathbf{p}) = \frac{\mathbf{p}\mathbf{p}^T}{|\mathbf{p}|^3}$ is singular with $\ker \mathbf{b}(\mathbf{p}) = \mathbf{p}^\perp$. Let $\mathbf{v} \in \ker \mathbf{b}(\mathbf{p})$; then

$$\mathbf{M}(\mathbf{p})\mathbf{v} = a_1(|\mathbf{p}|)\mathbf{v},$$

showing that $\mathbf{v}$ is an eigenvector of $\mathbf{M}(\mathbf{p})$ with eigenvalue $a_1(|\mathbf{p}|) = \frac{|\mathbf{p}|-1}{|\mathbf{p}|}$. It follows that $\operatorname{span} \mathbf{p}$ is an eigenspace, and we easily show that

$$\mathbf{M}(\mathbf{p})\mathbf{p} = \mathbf{p},$$

and 1 is the corresponding eigenvalue. We have shown that λ is an eigenvalue of $\mathbf{M}(\mathbf{p})$ if and only if

$$\lambda = \begin{cases} 1, & \text{algebraic multiplicity} = 1, \\ \frac{|\mathbf{p}|-1}{|\mathbf{p}|}, & \text{algebraic multiplicity} = 2, \end{cases} \tag{39}$$

with corresponding eigenspaces

$$\begin{aligned} E(1) &= \text{span}\,(\mathbf{p}), \\ E\left(\tfrac{|\mathbf{p}|-1}{|\mathbf{p}|}\right) &= \mathbf{p}^{\perp} = \{\mathbf{v} \in \mathbb{R}^3 | \mathbf{v} \cdot \mathbf{p} = 0\}. \end{aligned} \tag{40}$$

The matrix $\mathbf{M}(\mathbf{p})$ is therefore positive definite if and only if $|p| > 1$ and, in particular, the system of equations changes type when $|\partial_s \mathbf{r}| = 1$. It is *hyperbolic* when $|\partial_s \mathbf{r}| > 1$, whereas it will have components that are *elliptic* when $|\partial_s \mathbf{r}| < 1$. The Euler–Tricomi equation [27] is a linear system that exhibits a similar change of type in part of the phase space, and in general one expects loss of regularity, *a shock*, when $|\partial_s \mathbf{r}|$ moves through the unit circle.

This qualitative analysis suggests the *ill-posedness* of the classical tether equations. This ill-posedness will particularly hamper numerical integration. One can, for example, not expect conservation of energy through a shock. A drift in energy is indeed observed in the numerical computations in [20, 21] along with apparent tether discontinuities. In [15] we investigate the effect of the regularization in numerical integration for similar parameter values. The experiments show that using the regularization we can produce a more reliable integrator without a secular energy drift.

In the following section we conjecture that the slack-spring model is a limit of the massive tether model as the diameter of a stiff tether goes to 0. This will also force $EI \to 0$.

4. The vanishing thickness limit. Tethers are thin and longitudinally stiff. It therefore seems relevant to study the limit of vanishing thickness together with an assumption on the stiffness. Let h denote the diameter of a tether with constant circular cross-section such that $A = \frac{\pi}{4}h^2$, $\rho_l = \frac{\pi}{4}h^2\rho$, and $I = \frac{\pi}{64}h^4$. Then (13) may be written as

$$\frac{\pi}{4}h^2\rho\partial_t^2\mathbf{r} = -\mu\frac{\pi}{4}h^2\rho|\mathbf{r}|^{-3}\mathbf{r} + \frac{\pi}{4}Eh^2\partial_s\left(a_1(|\partial_s\mathbf{r}|)\partial_s\mathbf{r}\right) - \frac{\pi}{64}Eh^4\partial_s^4\mathbf{r}.$$

Now, if we assume that $E = \widehat{E}h^{-2}$ and normalize appropriately, we have

$$h^2\left(\partial_t^2\mathbf{r} + \partial_s^4\mathbf{r}\right) = \partial_s\left(a_1(|\partial_s\mathbf{r}|)\partial_s\mathbf{r}\right) + h^2\mathbf{f}(\mathbf{r}) \tag{41}$$

together with

$$\left.\begin{aligned} d_t^2\mathbf{x} + \mathbf{f}(\mathbf{x}) &= \left(a_1(|\partial_s\mathbf{r}|_{s=0}|)\partial_s\mathbf{r}\right)|_{s=0} - h^2\partial_s^3\mathbf{r}|_{s=0}, \\ d_t^2\mathbf{y} + \mathbf{f}(\mathbf{y}) &= -\left(a_1(|\partial_s\mathbf{r}|_{s=1}|)\partial_s\mathbf{r}\right)|_{s=1} + h^2\partial_s^3\mathbf{r}|_{s=0}, \\ \mathbf{r}|_{s=0} &= \mathbf{x}, \quad \mathbf{r}|_{s=1} = \mathbf{y}, \\ \partial_s^2\mathbf{r}|_{s=0,1} &= 0. \end{aligned}\right\} \tag{42}$$

The assumption that $E = \mathcal{O}(h^{-2})$ is appropriate since the boundary terms

$$\left(a_1(|\partial_s\mathbf{r}|_{s=0,1}|)\partial_s\mathbf{r}\right)|_{s=0,1}$$

are explicitly independent of h. For any other polynomial relation these terms would either vanish or diverge upon equating $h = 0$. By Theorem 1, this system admits a unique local solution for every $h > 0$. As mentioned, we can guarantee global existence only if singularities are not encountered. To avoid having to deal with the possibility that the solution in general exists only locally, we shall in the following replace $\mathbf{f}$ and a_1 by smooth mollifications $\mathbf{f}^{\mathrm{mol}}(\mathbf{z}) = \chi_\delta(|\mathbf{z}|)\mathbf{f}(\mathbf{z})$ and $a_1^{\mathrm{mol}}(z) = \chi_\delta(z)a_1(z)$, respectively, where $\chi_\delta : [0,\infty) \to [0,1]$ is a smooth function satisfying

$$\chi_\delta(z) = 1 \quad \text{whenever} \quad z \geq \delta$$

and

$$\begin{aligned} \chi_\delta(z) &\leq 1 \quad \text{whenever} \quad \delta/2 \leq z \leq \delta, \\ \chi_\delta(z) &= 0 \quad \text{whenever} \quad 0 \leq z \leq \delta/2 \end{aligned}$$

for some (small) $\delta > 0$.

The limit $h \to 0$ is singular. Our hope is that as $h \to 0$ the solution of (41) and (42) will converge to some sort of weak solution. The full weak solution will not be well defined; indeed, we lose all possible W^4-estimates on $\mathbf{r}$ as $h \to 0$. Nonetheless, we conjecture that the behavior of the boundaries *is* well defined and in particular that for certain initial conditions it converges as $h \to 0$ to that of the solution of the slack-spring problem.

Conjecture 1. *For $h > 0$ let $\boldsymbol{x}^h$ and $\boldsymbol{y}^h$ solve the boundary equations of (41) and (42) with initial conditions*

$$(\boldsymbol{x}(0), \boldsymbol{y}(0)) = (\boldsymbol{x}_0, \boldsymbol{y}_0) \in \mathbb{R}^6 \backslash \{0\}, \tag{43}$$

$$(\dot{\boldsymbol{x}}(0), \dot{\boldsymbol{y}}(0)) = (\dot{\boldsymbol{x}}_0, \dot{\boldsymbol{y}}_0) \in \mathbb{R}^6, \tag{44}$$

$$(\boldsymbol{u}(0), \boldsymbol{v}(0)) = (\boldsymbol{u}_0, \boldsymbol{v}_0) \tag{45}$$

satisfying

$$|\partial_s \boldsymbol{r}_0| = |\partial_s \boldsymbol{u}_0 + (\boldsymbol{y}_0 - \boldsymbol{x}_0)| = 1 \quad \textit{if} \quad |\boldsymbol{x}_0 - \boldsymbol{y}_0| < 1, \tag{46}$$

$$\boldsymbol{u}_0 = 0 \quad \textit{if} \quad |\boldsymbol{x}_0 - \boldsymbol{y}_0| \geq 1. \tag{47}$$

Let $\boldsymbol{x}$, $\boldsymbol{y}$ be the solutions of the slack-spring model

$$\begin{aligned} d_t^2 \boldsymbol{x} &= \boldsymbol{f}^{mol}(\boldsymbol{x}) + \widehat{a}_1(|\boldsymbol{y} - \boldsymbol{x}|)(\boldsymbol{y} - \boldsymbol{x}), \\ d_t^2 \boldsymbol{y} &= \boldsymbol{f}^{mol}(\boldsymbol{y}) + \widehat{a}_1(|\boldsymbol{y} - \boldsymbol{x}|)(\boldsymbol{x} - \boldsymbol{y}), \end{aligned}$$

with initial conditions (43) and (44). Then for almost all initial conditions

$$|(\boldsymbol{x}^h, \boldsymbol{y}^h)(t) - (\boldsymbol{x}, \boldsymbol{y})(t)|_{\mathbb{R}^6} = \mathcal{O}(h) \quad \textit{for} \quad 0 \leq t \leq \mathcal{O}(h^{-p}), \quad \textit{for some} \quad p > 0.$$

We aim to give a rigorous proof of this in future work. Here we argue from a qualitative perspective that the assertion seems reasonable. Equating $h = 0$ in (41), we obtain an ordinary differential equation,

$$\partial_s \left(a_1(|\partial_s \mathbf{r}|)\partial_s \mathbf{r} \right) = 0,$$

implying

$$a_1(|\partial_s \mathbf{r}|)\partial_s \mathbf{r} = \mathbf{const} \in \mathbb{R}^3,$$

and

$$|\partial_s \mathbf{r}| = \text{const} + 1,$$

with const $= |\mathbf{const}|$. We obtain, by assuming $|\partial_s \mathbf{r}| \neq 0$, that

$$|\partial_s \mathbf{r}| \equiv 1 \quad \text{for const} = 0, \tag{48}$$

$$\mathbf{u} = 0 \quad \text{for const} \neq 0. \tag{49}$$

The former is not possible when the satellites are separated by a distance greater than $l = 1$, while the latter is not stable in the sense of Euler buckling when $|\mathbf{y}-\mathbf{x}| < l$ [3]. To demonstrate Euler buckling we imagine $\mathbf{x}$ and $\mathbf{y}$ are fixed along the first inertial axis in free space, i.e., $\mathbf{f} = 0$, in the plane with $\mathbf{x} = (0, 0)$ and $\mathbf{y} = (1 - d, 0)$, $d < 1$. We are left with

$$h^2 \left(\partial_t^2 \mathbf{r} + \partial_s^4 \mathbf{r}\right) = \partial_s \left(a_1(|\partial_s \mathbf{r}|)\partial_s \mathbf{r}\right),$$

$\mathbf{r}|_{s=0} = 0$, $\mathbf{r}|_{s=1} = (1 - d, 0)$, and $\partial_s^2 \mathbf{r}|_{s=0,1} = 0$. Linearization about the compressed equilibrium $\mathbf{r} = ((1 - d)s, 0)$ gives

$$h^2 \left(\partial_t^2 \mathbf{r} + \partial_s^4 \mathbf{r}\right) = \text{diag}(1, -d/(1 - d))\partial_s^2 \mathbf{r}.$$

Through the ansatz $(r_1^{(n)}, r_2^{(n)})$, $r_i^{(n)} = \exp(i\varpi_i^{(n)} t)\sin(n\pi s)$, $i = 1, 2$, we obtain

$$\left(\varpi_2^{(n)}\right)^2 = -d/(1 - d)h^{-2}(\pi n)^2 + (\pi n)^4.$$

Solving $\varpi_2^{(n)} = 0$ for $h = h(d, n)$ gives a critical thickness,

$$h_{\text{crit}} = \frac{1}{\pi n}\sqrt{\frac{d}{1 - d}},$$

in the sense that $h < h_{\text{crit}}$ implies that the nth eigenmode is unstable. Finally, notice that $h_{\text{crit}} \to \infty$ for $d \to 1$, for fixed n.

If $|\partial_s \mathbf{r}| \equiv 1$, then the tether does not affect the motion of $\mathbf{x}$ and $\mathbf{y}$. This follows from the definition of a_1 and by differentiating $|\partial_s \mathbf{r}| \equiv 1$ twice and using the boundary conditions $\partial_s^2 \mathbf{r}|_{s=0,1} = 0$. On the other hand, when $\mathbf{u} = 0$, or $\mathbf{r} = s\mathbf{y} + (1 - s)\mathbf{x}$, the boundary terms, entering the equations for $\mathbf{x}$ and $\mathbf{y}$, equal the effect of a spring with stiffness 1 connecting the two satellites.

The buckling result does not imply the nonexistence of compressed tether motion. Certainly, zero angular momentum solutions provide a counterexample. However, we believe that the buckling result will imply that the set of initial conditions for which the result is not true is *small* in some sense. This is the reason for the phrase *for almost initial conditions*. In the construction of a rigorous proof this phrase and proper estimates on the convergence rate p will have to be made precise.

We will now revisit the slack-spring model and introduce the billiard model as the limit of an inextensible spring.

5. The slack-spring model.

5.1. Linearization of the gravitational field. The slack-spring model with Hamiltonian (19), repeated here for convenience,

$$H_{\mathrm{ST}}(\mathbf{q},\boldsymbol{\delta q},\mathbf{p},\boldsymbol{\delta p}) = \frac{1}{2\xi}|\mathbf{p}|^2 + \frac{1}{2}|\boldsymbol{\delta p}|^2 - \frac{1}{\mu_{\mathbf{x}}}\frac{\mu}{|\mathbf{q}+\mu_{\mathbf{x}}\boldsymbol{\delta q}|} - \frac{1}{\mu_{\mathbf{y}}}\frac{\mu}{|\mathbf{q}-\mu_{\mathbf{y}}\boldsymbol{\delta q}|} + \kappa \mathbf{1}_{|\boldsymbol{\delta q}|-l}\left(|\boldsymbol{\delta q}|-l\right)^2, \tag{50}$$

is 12-dimensional. In section 2.2, restricting to planar dynamics and introducing appropriate polar coordinates, we were able to reduce to 3 degrees of freedom; see (20). However, even 6 dimensions are too many to easily visualize the dynamics. To overcome this problem we may make use of the fact that in practice $l \ll r$ and in particular replace the gravitational term in Hamilton's equations with its linearized versions about $\boldsymbol{\delta q} = 0$. We obtain

$$\begin{aligned}
\dot{\mathbf{q}} &= \frac{1}{\xi}\mathbf{p},\\
\dot{\mathbf{p}} &= -\frac{1}{\xi}\frac{\mu}{|\mathbf{q}|^3}\mathbf{q},\\
\dot{\boldsymbol{\delta q}} &= \boldsymbol{\delta p},\\
\dot{\boldsymbol{\delta p}} &= -\frac{\mu}{|\mathbf{q}|^3}\left(I - 3\frac{\mathbf{q}\mathbf{q}^T}{|\mathbf{q}|^2}\right)\boldsymbol{\delta q} - 2\kappa\widehat{a}_l(|\boldsymbol{\delta q}|)\boldsymbol{\delta q}.
\end{aligned}$$

Within this approximation the center of mass is independent of the relative motion and moves on a Keplerian orbit. The Keplerian motion conserves eccentricity e, and for $0 \le e < 1$ the motion is bounded and periodic. We therefore replace the original Hamiltonian system with a family of time-periodic Hamiltonians parametrized by $e \in [0,1)$. If we introduce the true anomaly ν in Figure 2 as an independent variable and normalizations such that $\dot{\nu} = (1+e\cos\nu)^2$ and $l = 1$, then the Hamiltonian takes the form

$$H_{\mathrm{ST}}(\boldsymbol{\delta q},\boldsymbol{\delta p},\nu;e) = \frac{1}{2\dot{\nu}}|\boldsymbol{\delta p}|^2 - \frac{1}{2}(1+e\cos\nu)\langle \boldsymbol{\delta q}, \mathbf{A}(\nu)\boldsymbol{\delta q}\rangle + \frac{\kappa}{\dot{\nu}}\mathbf{1}_{|\boldsymbol{\delta q}|-l}\left(|\boldsymbol{\delta q}|-l\right)^2, \tag{51}$$

where

$$\mathbf{A}(\nu) = \mathbf{I} - 3\begin{pmatrix} \cos^2\nu & \sin\nu\cos\nu & 0\\ \sin\nu\cos\nu & \sin^2\nu & 0\\ 0 & 0 & 0\end{pmatrix}.$$

Finally, by moving into a rotating frame,

$$\begin{aligned}
\boldsymbol{\delta q} &= \mathbf{R}(\nu)\boldsymbol{\delta q}^{\mathrm{rot}},\\
\boldsymbol{\delta p} &= \mathbf{R}(\nu)\boldsymbol{\delta p}^{\mathrm{rot}},
\end{aligned}$$

where $\mathbf{R}(\nu) \in \mathrm{SO}(3)$ for every ν,

$$\mathbf{R}(\nu) = \begin{pmatrix} \cos\nu & -\sin\nu & 0\\ \sin\nu & \cos\nu & 0\\ 0 & 0 & 1\end{pmatrix},$$

we obtain a new Hamiltonian as the sum of the old one written in the new variables and the coriolis term $\langle \boldsymbol{\delta}\mathbf{q}^{\mathrm{rot}}, \boldsymbol{\Omega} \wedge \boldsymbol{\delta}\mathbf{p}^{\mathrm{rot}} \rangle$:

$$
\begin{aligned}
H_{\mathrm{ST}}(\boldsymbol{\delta}\mathbf{q}^{\mathrm{rot}}, \boldsymbol{\delta}\mathbf{p}^{\mathrm{rot}}, \nu; e) = \frac{1}{2\dot{\nu}} |\boldsymbol{\delta}\mathbf{p}^{\mathrm{rot}}|^2 + \langle \boldsymbol{\delta}\mathbf{q}^{\mathrm{rot}}, \boldsymbol{\Omega} \wedge \boldsymbol{\delta}\mathbf{p}^{\mathrm{rot}} \rangle \\
+ (1 + e\cos\nu) \left((\delta q_1^{\mathrm{rot}})^2 - \frac{1}{2}(\delta q_2^{\mathrm{rot}})^2 - \frac{1}{2}(\delta q_3^{\mathrm{rot}})^2 \right) \\
+ \frac{\kappa}{\dot{\nu}} \mathbf{1}_{|\boldsymbol{\delta}\mathbf{q}^{\mathrm{rot}}|-1} (|\boldsymbol{\delta}\mathbf{q}^{\mathrm{rot}}| - 1)^2,
\end{aligned} \tag{52}
$$

where $\boldsymbol{\delta}\mathbf{q}^{\mathrm{rot}} = (\delta q_1^{\mathrm{rot}}, \delta q_2^{\mathrm{rot}}, \delta q_3^{\mathrm{rot}})^T$, $\boldsymbol{\delta}\mathbf{p} = (\delta p_1^{\mathrm{rot}}, \delta p_2^{\mathrm{rot}}, \delta p_3^{\mathrm{rot}})^T$, and $\boldsymbol{\Omega} = (0, 0, 1)$.

The Hamiltonian $H_{\mathrm{ST}}(\boldsymbol{\delta}\mathbf{q}^{\mathrm{rot}}, \boldsymbol{\delta}\mathbf{p}^{\mathrm{rot}}, \nu; 0)$, corresponding to a circular orbiting center of mass, is independent of ν, and H_{ST} is conserved. The six dimensional phase space is therefore foliated by five dimensional submanifolds, or three dimensional submanifolds if we restrict to planar motion. In the latter case visualizations are possible with two dimensional Poincaré maps.

In the dumbbell model the distance between the spacecraft is assumed constant and equal to $l = 1$. Therefore, by replacing the Euclidean configuration space above with S^2 for the attitude of the dumbbell, we obtain the dumbbell model with linearized gravity; see, e.g., [10]. For $e = 0$ and restricting to planar motion we obtain a time-independent one degree of freedom integrable Hamiltonian system. We shall return to this "underlying" integrable system when we later identify the dumbbell dynamics within the billiard dynamics. We mention that for the dumbbell model with small e most of the invariant curves of the planar dumbbell dynamics will persist by considering the stroboscopic, symplectic map and using KAM theory.

5.2. The inextensible limit of the slack-spring model. Our aim in this subsection is to study the inextensible limit of the slack-spring model. We will show that the impact of $\boldsymbol{\delta}\mathbf{q}$ with $|\boldsymbol{\delta}\mathbf{q}| = 1$ approximates a δ-distribution as $\kappa \to \infty$, the effect of which is to reverse the direction of the radial momentum, $p_{\delta r} \mapsto -p_{\delta r}$, leaving the remaining variables continuous in time.

The slack-spring problem can be viewed as a hybrid system: an integrable Hamiltonian flow within $|\boldsymbol{\delta}\mathbf{q}^{\mathrm{rot}}| \leq 1$ and a different flow beyond where the spring affects the motion. Since the flow within $|\boldsymbol{\delta}\mathbf{q}^{\mathrm{rot}}| < 1$ is not affected by the spring, or the value of κ, for the purpose of our study it suffices to study the region $|\boldsymbol{\delta}\mathbf{q}^{\mathrm{rot}}| \geq 1$. To do so we consider the related spring system, i.e., replacing $\widehat{a}_1$ (18) by a_1 (10). We assume $e = 0$ and restrict to planar dynamics for simplicity. The arguments can easily be extended for $0 < e < 1$ and the nonplanar case.

We introduce the polar coordinates $\boldsymbol{\delta}\mathbf{q}^{\mathrm{rot}} = \delta r(\cos\theta, \sin\theta)$. Upon replacing $\widehat{a}_1$ by a_1, Hamilton's equations, with Hamiltonian (52), become

$$
\begin{aligned}
\ddot{\delta r} &= \delta r \dot{\theta}^2 + 3\delta r \cos(\theta)^2 + 2\kappa(1 - \delta r) + 2\delta r \dot{\theta}, \\
d_t \left(\delta r^2 \dot{\theta} \right) &= -3\delta r^2 \cos(\theta)\sin(\theta) - 2\delta r \dot{\delta r}.
\end{aligned} \tag{53}
$$

We introduce the slow time $\tau = \epsilon^{-1} t$ and set $\delta r(\tau) = 1 + \epsilon \delta r_1(\tau)$ with $\epsilon^2 = \kappa^{-1}$ to obtain

$$
\begin{aligned}
\delta r_1'' &= -2\delta r_1 + \mathcal{O}(\epsilon), \quad ()' = d_\tau, \\
\ddot{\theta} &= -3\cos(\theta)\sin(\theta) + \mathcal{O}(\epsilon).
\end{aligned}
$$

Therefore, if $\delta r_1(0) = 0$ with $\dot{\delta r}_1(0) = B$, then after truncating terms of order ϵ,

$$\delta r_1(t) = B \sin(\sqrt{2\kappa} t),$$

and it follows that the effect of moving beyond $\delta r = 1$ is approximated by the *bounce map* $\dot{\delta r} \mapsto -\dot{\delta r}$, leaving the other variables, $\delta r, \theta$, and $\dot{\theta}$, continuous. Together the bounce map and the Keplerian flow between bounces define the billiard model.

The Kelvin–Voigt dissipation enters on the right-hand side of (53) via the term $-2\kappa\alpha\dot{\delta r}$. If we assume that the damping factor is small and in particular satisfy $\alpha = \tilde{\alpha}\epsilon$ for some $\tilde{\alpha} \in [0, 2)$, then the calculations made above can be repeated to show that the truncation satisfies

$$\delta r_1'' = -2\delta r_1 - 2\tilde{\alpha}\delta r_1'.$$

Therefore,

$$\delta r_1 = \frac{B}{\sqrt{2 - \tilde{\alpha}}} \exp\left(-\tilde{\alpha}\sqrt{\kappa} t\right) \sin\left(\sqrt{2 - \tilde{\alpha}^2}\sqrt{\kappa} t\right),$$

so that in the limit of $\epsilon = 0$

$$\dot{\delta r} \mapsto -\dot{\delta r} \exp\left(-\frac{\tilde{\alpha}\pi}{\sqrt{2 - \tilde{\alpha}}}\right) = -\dot{\delta r}\left(1 - \frac{\pi}{\sqrt{2}}\tilde{\alpha} + \mathcal{O}(\tilde{\alpha}^2)\right).$$

The dissipation can therefore be accounted for within the billiard model via the restitution factors $\exp(-\frac{\tilde{\alpha}\pi}{\sqrt{2-\tilde{\alpha}}})$. This is done in [30]. This reference considers a fixed circular orbiting center of mass and shows numerically that, as might be expected for a nonlinear, almost Hamiltonian system, transient chaos before the system converges to the stable equilibria.

In the following section the billiard model is studied further. The overall aim shall be to identify the dumbbell dynamics within the dynamics of the billiard model.

6. The billiard model. Between collisions the flow is given by the Hamiltonian

$$\begin{aligned} Q((\boldsymbol{\delta q}^{\mathrm{rot}}, \nu), (\boldsymbol{\delta p}^{\mathrm{rot}}, \mathcal{E}); e) = \mathcal{E} + \frac{1}{2\dot{\nu}}|\boldsymbol{\delta p}^{\mathrm{rot}}|^2 + \langle \boldsymbol{\delta q}^{\mathrm{rot}}, \boldsymbol{\Omega} \wedge \boldsymbol{\delta p}^{\mathrm{rot}} \rangle \\ - (1 + e\cos\nu)\left((\delta q_1^{\mathrm{rot}})^2 - \frac{1}{2}(\delta q_2^{\mathrm{rot}})^2 - \frac{1}{2}(\delta q_3^{\mathrm{rot}})^2\right), \end{aligned} \tag{54}$$

with canonical symplectic structure $\omega = d\boldsymbol{\delta q}^{\mathrm{rot}} \wedge \boldsymbol{\delta p}^{\mathrm{rot}} + d\nu \wedge d\mathcal{E}$. This is just (52) without the slack-spring term and where we have introduced the negative energy $\mathcal{E}$ as the canonical conjugate of ν. Recall that $\boldsymbol{\Omega} = (0, 0, 1)$. This Hamiltonian is integrable as it is obtained from the variations of the integrable Kepler problem. In fact, for $0 \le e < 1$ there is a five dimensional family of periodic solutions of the variational equations [14]. By linearity these solutions can be scaled such that they never intersect $|\boldsymbol{\delta q}^{\mathrm{rot}}| = 1$. This set of solutions is an integrable periodic subset of the billiard dynamics. The sixth remaining solution of the variational equations is a linear drift due to variations in energy [14]. We consider initial conditions for the billiard map on $|\boldsymbol{\delta q}^{\mathrm{rot}}| = 1$. If these initial conditions correspond to a periodic solution of the variational equations, then the relative position vector certainly returns

to $|\boldsymbol{\delta q}^{\rm rot}| = 1$. Otherwise, by the linear drift, the relative position is radially expanding. It therefore follows that every point on the section $|\boldsymbol{\delta q}^{\rm rot}| = 1$ for which $d_t|\boldsymbol{\delta q}^{\rm rot}| < 0$ is mapped through the flow of (54) to a point on $|\boldsymbol{\delta q}^{\rm rot}| = 1$ with $d_t|\boldsymbol{\delta q}^{\rm rot}| > 0$. This defines a map B_e, parametrized by the eccentricity e, mapping wall-collisions to wall-collisions. Since $p_{\delta r} \mapsto -p_{\delta r}$ leaves Q invariant and Q, as a time-independent Hamiltonian, is conserved on the integral curves between collisions, B_e maps the level sets of Q, $Q = \xi$, into themselves. Therefore,

$$B_e(\mathbf{z}_0, \xi) = (\mathbf{z}_1, \xi), \quad \mathbf{z}_0, \mathbf{z}_1 = \mathbf{z}_1(\mathbf{z}_0, \xi) \in T^*(S^2 \times S^1).$$

Here S^2 is for $|\boldsymbol{\delta q}^{\rm rot}| = 1$ measuring the collision attitude, while S^1 is for the true anomaly ν. As is usual for Hamiltonian Poincaré maps, the mapping

$$P_e : \mathbf{z}_0 \mapsto \mathbf{z}_1 \tag{55}$$

is smooth and symplectic on $T^*(S^2 \times S^1)$.

For $e = 0$ further reduction is possible. Indeed, in this case ν is cyclic in the Hamiltonian (54), and $\mathcal{E}$ is therefore conserved, say, $\mathcal{E} = c$. Hence

$$P_0(\mathbf{z}_0, \nu_0, c) = (\mathbf{z}_1, \nu_0 + \Delta\nu(\mathbf{z}_0, c), c), \quad \mathbf{z}_0, \mathbf{z}_1 = \mathbf{z}_1(\mathbf{z}_0, c) \in T^*S^2, \tag{56}$$

and we define $P_0^{c,\rm red} : \mathbf{z}_0 \mapsto \mathbf{z}_1$ with $\mathcal{E} = c$. This is a family of four dimensional smooth symplectic maps parametrized by c. The planar restriction defines a family of two dimensional symplectic maps on the cylinder T^*S^1.

6.1. The dumbbell motion. The dumbbell motion is embedded within the billiard model as trajectories grazing along the boundary. As already mentioned in the last paragraph of section 5.1, this dumbbell motion is integrable when restricted to planar motion and $e = 0$. The interesting question is when this specific dynamics persists for slack tethers or, in other words, when is it obtainable as a limit within the billiard map. The existence of these regions of persistence will provide subsets of phase space in which the dumbbell model will be a valid approximation to the full dynamics.

For $e = 0$ the ν-independence of Q allows us to identify $\mathcal{E}$ with the associated energy function. In polar coordinates we may then write $E = -\mathcal{E}$ as

$$E = \frac{1}{2}\dot{\delta r}^2 + \frac{1}{2}\delta r^2\dot{\theta}^2 - \frac{3}{2}\delta r^2\cos^2\theta. \tag{57}$$

We say that a frequency ω satisfies the *Diophantine condition* if there exist $\tau \geq 1$ and $C > 0$ such that $|n\omega - m| > Cn^{-\tau}$, $C > 0$ for any $n, m \in \mathbb{N}$. We then obtain the following theorem.

Theorem 2. *Any invariant curve of the dumbbell model with $e = 0$, $\lambda = \dot{\theta}^2 + 2\dot{\theta} + 3\cos^2\theta > 0$, and an induced frequency ω satisfying the Diophantine condition persists within the reduced billiard map.*

Proof. The proof is inspired by a proof of the existence of invariant curves in magnetic billiards in [8]. It goes as follows.

1° Obtain an approximation to the billiard map using the *escape velocity* as a small parameter.

2° Derive an area-preserving, twist-mapping approximation using canonical transformations.

3° Use Moser's twist theorem [24, Theorem 2.11] to conclude the existence of invariant curves near the boundary.

1°. In polar coordinates the Hamiltonian (54) with $e = 0$ reads

$$Q = \frac{1}{2}p_{\delta r}^2 + \frac{{p_\theta}^2}{2\delta r^2} - p_\theta + \frac{1}{2}\delta r^2 - \frac{3}{2}\delta r^2 \cos^2\theta,$$

equipped with $\omega = d\delta r \wedge dp_{\delta r} + d\theta \wedge dp_\theta$. As we will be considering trajectories grazing along the boundary $\delta r = 1$, we introduce ϵ and $\delta\tilde{r}$ so that $\delta r = 1 + \epsilon\delta\tilde{r}$. It is moreover appropriate to introduce $p_{\delta r} = \epsilon^{1/2}\tilde{p}_{\delta r}$ and $t \mapsto \epsilon^{-1/2}t$. Upon forgetting the tildes the Hamiltonian is transformed into

$$\begin{aligned} Q &= \frac{1}{2}\epsilon p_{\delta r}^2 + \frac{{p_\theta}^2}{2(1+\epsilon r)^2} - p_\theta + \frac{1}{2}(1+\epsilon\delta r)^2 - \frac{3}{2}(1+\epsilon\delta r)^2\cos^2\theta \\ &= \frac{1}{2}\epsilon p_{\delta r}^2 + h(\theta, p_\theta) - \epsilon\lambda(\theta, p_\theta)\delta r + \mathcal{O}(\epsilon^2), \end{aligned}$$

equipped with $\omega = \epsilon d\delta r \wedge dp_{\delta r} + \epsilon^{-1/2}d\theta \wedge dp_\theta$. Here

$$h(\theta, p_\theta) = \frac{1}{2}{p_\theta}^2 - p_\theta - \frac{3}{2}\cos^2\theta$$

is the Hamiltonian of the associated dumbbell model with $e = 0$, and

$$\lambda(\theta, p_\theta) = {p_\theta}^2 - 1 + 3\cos^2\theta,$$

which satisfies

$$-\epsilon^{-1}\partial_{\delta r}Q \to \lambda$$

as $\epsilon \to 0$.

Remark 1. The quantity $\lambda = \dot{\theta}^2 + 2\dot{\theta} + 3\cos^2\theta + \mathcal{O}(\epsilon)$ is the acceleration of δr. Physically (see, e.g., [4]), λ with $\epsilon = 0$ is the tension in the associated dumbbell required to keep it unit-speed parametrized. If λ is $\mathcal{O}(\epsilon^{1/2})$, or even $\lambda < 0$, then the estimates below are not valid. In particular, Hamilton's equations for δr and $p_{\delta r}$ are

$$\epsilon\dot{\delta r} = \epsilon p_{\delta r}, \tag{58}$$

$$\epsilon\dot{p_{\delta r}} = \epsilon\lambda + \mathcal{O}(\epsilon^2). \tag{59}$$

Therefore, if a trajectory is initiated on the boundary with $\delta r(0) = 0$ and $\dot{\delta r}(0) < 0$, then, within the truncation of these equations, δr will only return to 0 if $\lambda > 0$. See also Figure 4. However, we may notice that $\lambda \le 0$ gives $-1 - \sqrt{1 - 3\cos^2\theta} \le \dot{\theta} \le \sqrt{1 - 3\cos^2\theta} - 1 \le 0$, and therefore the negativity of λ is an issue only when the tethered system's rotation opposes the direction of rotation of the center of mass (retrograde orbits).

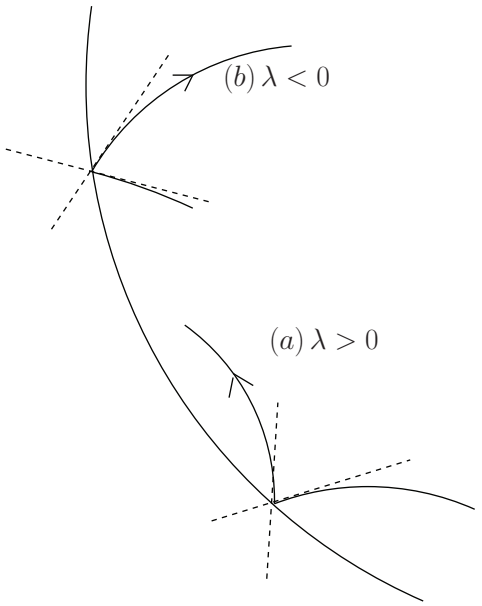

Figure 4. *If* (a) $\lambda > 0$*, then the trajectory remains close to the boundary provided the radial escape velocity* $p_{\delta r}$ *is sufficiently small. This is in general not the case for* (b) $\lambda < 0$.

We will assume for the moment that

$$\lambda \geq \delta > 0. \tag{60}$$

We will return to this in 2°. As the billiard map is symplectic on energy level sets, we will reduce by energy. To return to the boundary $p_{\delta r}$ will obviously have to chance sign, so we will eliminate δr rather than $p_{\delta r}$ via the conservation of energy

$$Q(\delta r, p_{\delta r}, \theta, p_\theta) = c. \tag{61}$$

We have

$$\partial_{\delta r} Q = -\epsilon\lambda + \mathcal{O}(\epsilon^2).$$

Therefore, for ϵ small enough, using the implicit function theorem and assumption (60), we can solve (61) for δr. Notice that $0 > h - c = \mathcal{O}(\epsilon)$. Let us therefore set $h - c = \epsilon\tilde{h}(\theta, p_\theta, c) < 0$. Moreover, let

$$\delta r = M_\epsilon(p_{\delta r}, \theta, p_\theta, c) = M_0(p_{\delta r}, \theta, p_\theta, c) + \epsilon M_1(p_{\delta r}, \theta, p_\theta, c) + \mathcal{O}(\epsilon^2).$$

By insertion we obtain

$$M_0 = \frac{\tilde{h}}{\lambda} + \frac{p_{\delta r}^2}{2\lambda}.$$

Next, we eliminate $p_{\delta r}$ which is conjugate to δr by replacing time with $p_{\delta r}$. We have

$$\frac{d\theta}{dp_{\delta r}} = -\epsilon^{3/2}\frac{\partial_{p_\theta} Q}{\partial_{\delta r} Q},$$
$$\frac{dp_\theta}{dp_{\delta r}} = \epsilon^{3/2}\frac{\partial_\theta Q}{\partial_{\delta r} Q}.$$

But from (61) it follows upon using the chain rule that

$$\partial_\theta Q + \partial_{\delta r} Q \partial_\theta M_\epsilon = 0,$$
$$\partial_{p_\theta} Q + \partial_{\delta r} Q \partial_{p_\theta} M_\epsilon = 0,$$

and therefore

$$\frac{d\theta}{dp_{\delta r}} = \partial_{p_\theta}\left(\epsilon^{3/2} M_\epsilon\right),$$
$$\frac{dp_\theta}{dp_{\delta r}} = -\partial_\theta\left(\epsilon^{3/2} M_\epsilon\right).$$

The reduced system is therefore Hamiltonian with Hamiltonian function $\epsilon^{3/2} M_\epsilon$ and symplectic form $d\theta \wedge dp_\theta$. Here

$$\epsilon^{3/2}\partial_z M_0 = \epsilon^{1/2}\frac{\partial_z h}{\lambda} - \epsilon^{3/2}\frac{\partial_z \lambda}{\lambda}\left(p_{\delta r}^2 + \tilde{h}\right), \quad z = \theta \text{ or } p_\theta.$$

Therefore,

$$\frac{d\theta}{dp_{\delta r}} = \epsilon^{1/2}\frac{\partial_{p_\theta} h}{\lambda} + \cdots,$$
$$\frac{dp_\theta}{dp_{\delta r}} = -\epsilon^{1/2}\frac{\partial_\theta h}{\lambda} + \cdots.$$

To approximate the billiard map the truncation of this system has to be integrated up until the trajectory returns to the boundary corresponding to $\delta r = 0$. In the following we approximate the required integration time. First we notice that from (61) it follows that on the boundary, given by $\delta r = 0$, we have $p_{\delta r} = -\frac{1}{2}N_0 + \mathcal{O}(\epsilon)$, $N_0 = 2\sqrt{-2\tilde{h}}$. Hence by (58) and (59), or

$$\ddot{\delta r} = \lambda + \mathcal{O}(\epsilon),$$

we obtain

$$\delta r = \frac{\lambda}{2}t^2 - \frac{1}{2}N_0 t + \mathcal{O}(\epsilon).$$

The equation $\delta r = 0$ to be solved for the return time $\Delta t > 0$ therefore solves to

$$\Delta t = \frac{N_0}{\lambda} + \mathcal{O}(\epsilon),$$

which is positive for sufficiently small ϵ since by assumption (60) $\lambda > 0$. In terms of $p_{\delta r}$ the return time becomes $\Delta p_{\delta r} = N_0 + \mathcal{O}(\epsilon)$. If $\tau = \frac{p_{\delta r}}{N_0}$ is a new time, then the return time becomes

$$\Delta\tau = 1 + \mathcal{O}(\epsilon), \tag{62}$$

and the equations read

$$\begin{aligned} \frac{d\theta}{d\tau} &= \epsilon^{1/2}\frac{\partial_{p_\theta} h}{N_0\lambda} + \cdots, \\ \frac{dp_\theta}{d\tau} &= -\epsilon^{1/2}\frac{\partial_\theta h}{N_0\lambda} + \cdots. \end{aligned} \tag{63}$$

2°. The truncation of (63) is a time reparametrization of the dumbbell model with Hamiltonian h, and according to (62) its time-one map approximates the billiard map. Notice also that the truncation preserves N_0 since it conserves h. Therefore, in terms of the action-angle variables (ϕ, J) of the dumbbell, the truncation of (63) reads

$$\begin{aligned} \dot{\phi} &= \frac{\epsilon^{1/2}}{N_0\lambda}\varpi(J), \\ \dot{J} &= 0. \end{aligned}$$

Now, introduce $\phi \mapsto \psi$, where

$$\psi = \frac{\int_0^\phi \lambda(\tau, J)d\tau}{\overline{\lambda}}, \quad \overline{\lambda} = \frac{1}{2\pi}\int_0^{2\pi} \lambda(\tau, J)d\tau,$$

and $\epsilon \mapsto \tilde{\epsilon} = \epsilon N_0^2$. The new $\tilde{\epsilon}$ is still small since $N_0 = \mathcal{O}(1)$ and the truncation preserves it. Then the equations are transformed into

$$\begin{aligned} \dot{\psi} &= \tilde{\epsilon}^{1/2}\varpi(J), \\ \dot{J} &= 0. \end{aligned}$$

Since the dumbbell model with $e = 0$ is just a pendulum equation, the time-one map of the dumbbell obviously satisfies the twist condition $\partial_J \varpi(J) \neq 0$ [24] away from the separatrices. It is therefore only left to be shown that (60) holds in parts of the phase space. We may write

$$\begin{aligned} \lambda &= 2\eta + 6\cos^2\theta + 2\dot{\theta}(\theta, \eta) \\ &= 2\eta + 6\cos^2\theta \pm 2\sqrt{2\eta + 3\cos^2\theta}, \end{aligned}$$

where $2\eta = \dot{\theta}^2 - 3\cos^2\theta$ is the energy function related to h and therefore conserved. At the $\theta = 0, \pi$ equilibria, $\eta = -3/2$ and therefore $\lambda = 3$. Moreover, $\lambda > 0$ for sufficiently large η.

3°. For $\lambda > 0$ we have an area-preserving approximation of the billiard map through the time-one map of the truncation of the map (63). Moser's twist map theorem then guarantees the persistence of Diophantine tori. ∎

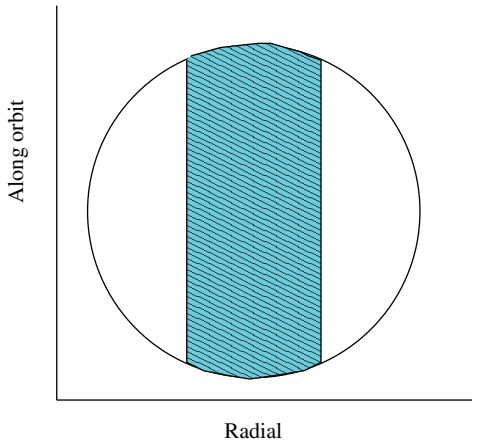

Figure 5. *The two white, disjoint regions sketch the realm of possible motion for $E < 0$.*

Remark 2. The arguments can also be repeated for a more general class of linear time-independent Hamiltonian vector-fields describing the flow between collisions. Another example could be the variational equations about the collinear Lagrange points in the circular restricted three-body problem. Moreover, similar techniques have been used in magnetic billiards; see, e.g., [8].

The tori which do not persist the perturbation, in particular tori with rational frequencies, break up into island chains and chaos [2]. In the following section we show some diagrams of numerical computations of the billiard map, particularly bringing attention to the dynamics away from the KAM tori.

6.2. Numerical computations of the billiard map for $e = 0$. We focus our attention on $e = 0$ and the family of two dimensional billiard maps describing the planar billiard dynamics. Again we use θ and $\dot{\theta}$ as coordinates on the cylinder TS^1; see, Figure 2 for the definition of θ.

The invariant sets defined by $E = c$ (57) are disconnected for $E < 0$. For $E < 0$ the dynamics are confined to two regions of configuration space: $|\delta r \cos\theta| \geq \sqrt{-\frac{3}{2}E}$; see Figure 5. For $E \geq 0$ any point of configuration space, $\delta r \leq 1$, can be visited by the dynamics. In particular, collisions between the satellites can occur if and only if $E \geq 0$. The topology of the sets $E^{-1}(c)$, with $c \geq -\frac{3}{2}$, obviously implies that the billiard mapping is defined only on a proper subset of $(-\pi, \pi] \ni \theta$.

Figure 6 shows four examples of the billiard map restricted to the level sets of E. In Figure 6 (a), (b), (c), and (d) E is fixed at -0.7, 0.1, 1, and 5. On the boundary curves, $\dot{\delta r} = 0$, i.e., the dumbbell limit. Due to reflectional symmetries about the lines $\theta = 0$ and $\theta = \pi/2$ the sections with θ in only one of the regions $(0, \pi/2)$, $(\pi/2, \pi)$, $(-\pi, -\pi/2)$, and $(-\pi/2, 0)$ uniquely define the billiard map.

There is an obvious difference in the dynamics of direct and retrograde orbits, i.e., $\dot{\theta} > 0$ and $\dot{\theta} < 0$, respectively. Similar differences can be observed in the circular restricted three-body problem in rotating coordinates, or in magnetic billiards [8]. In general, retrograde orbits have more energy as they need to be faster to reach the next collision.

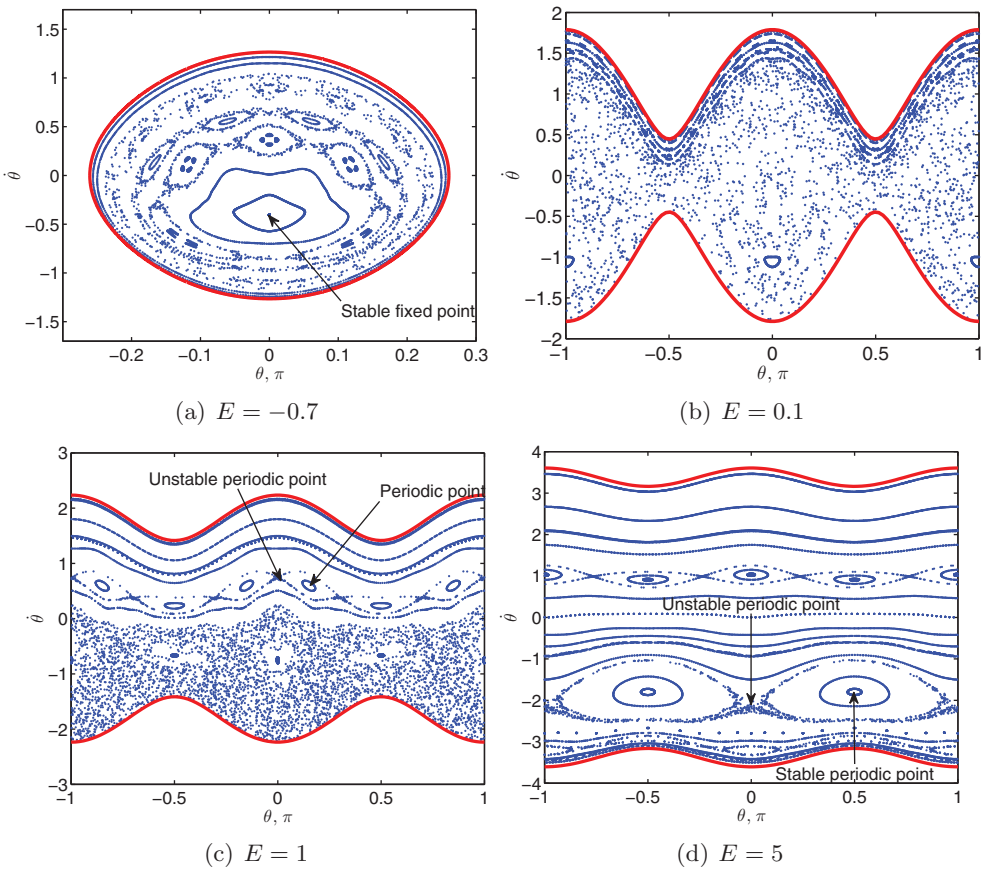

(a) $E = -0.7$ (b) $E = 0.1$

(c) $E = 1$ (d) $E = 5$

Figure 6. *Visualization of the billiard map for E-values equal to -0.7, 0.1, 1, and 5. On the boundary curves $\dot{\delta r} = 0$, i.e., the dumbbell limit. The periodic points pointed out by the arrows in* (a), (c), *and* (d) *are visualized as projections of periodic orbits in Figure 7.*

In (a), $E = -0.7$, there are two obvious dominating regular regions: invariant curves near the boundary and an elliptic island. Between these regions we see both chaotic regions and additional smaller regular islands. The large elliptic island surrounds a nonlinear normal mode emerging from the stable fixed point. As E is increased, the qualitative picture in Figure 6 (a) persists until $E = 0$, where the two white regions in Figure 5 collide to enable transfer between the two half discs. Immediately after $E = 0$, the dynamics is predominantly chaotic; see Figure 6 (b). Increasing the energy to $E = 1$ regularizes the dynamics near the top boundary, and resonance islands appear; see Figure 6 (c). Increasing the energy even further to $E = 5$ (Figure 6 (d)) regularizes the dynamics near the lower boundary, again creating resonance islands. The behavior of the invariant curves near the boundary is in agreement with Theorem 2 and Remark 1.

Projections of the five periodic orbits identified with periodic and fixed points for the billiard map (see Figure 6) are visualized in Figure 7. By the implicit function theorem, periodic and fixed points can be continued onto neighboring energy surfaces provided 1 is not an eigenvalue of the linearized map. In Figure 7 (a), the stable fixed point visible in Figure 6 (a) has been continued for E near -0.7.

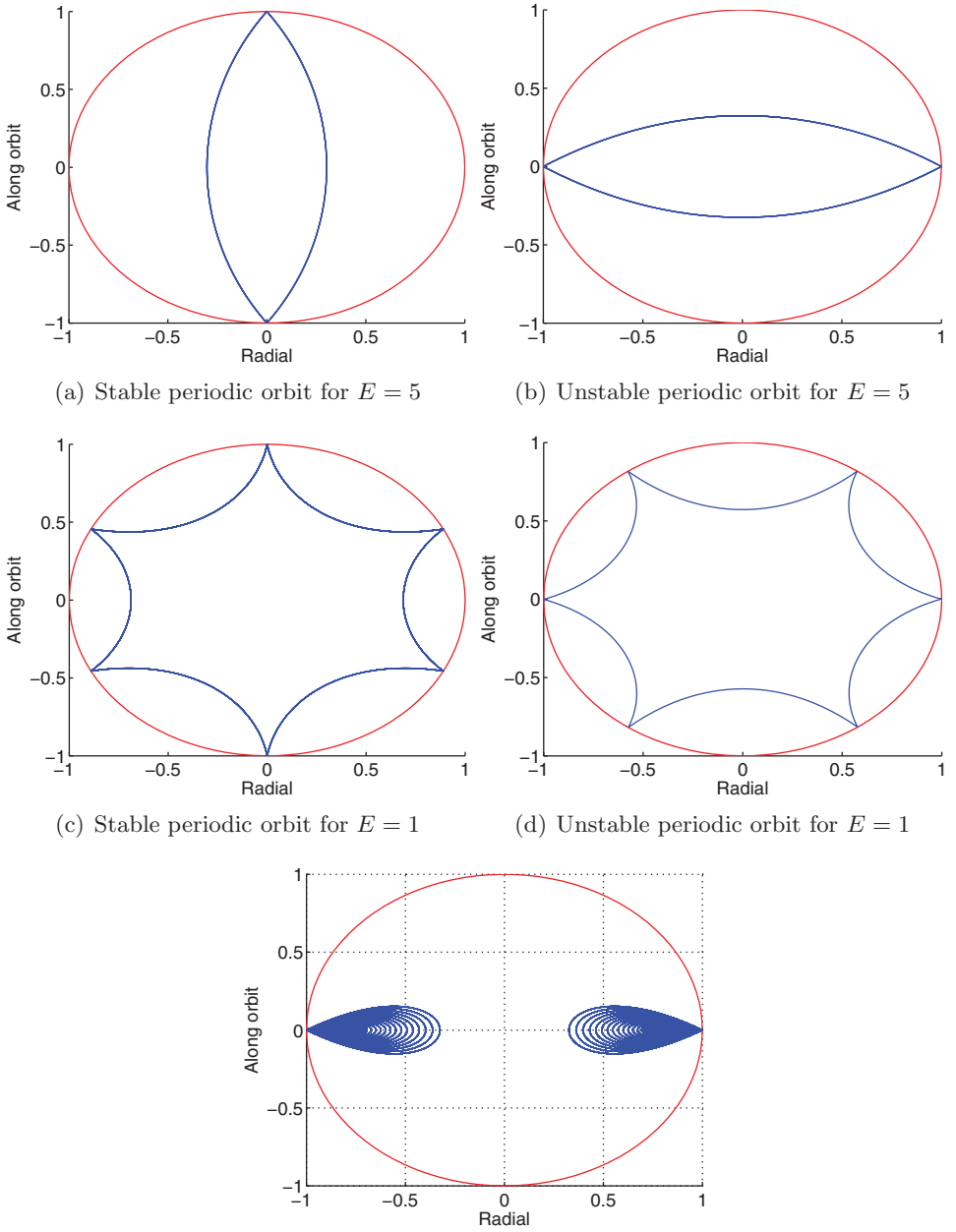

(a) Stable periodic orbit for $E = 5$

(b) Unstable periodic orbit for $E = 5$

(c) Stable periodic orbit for $E = 1$

(d) Unstable periodic orbit for $E = 1$

(e) Family of stable periodic orbits for E near -0.7

Figure 7. *The periodic orbits corresponding to the periodic points of the billiard map indicated in Figure 6. Unstable and stable periodic orbits are visualized. By the implicit function theorem, the periodic points can be continued onto neighboring energy surfaces.*

The invariant curves near the boundaries are codimension 1, and they therefore act as absolute barriers to the motion. In particular, for these reasons, trajectories emanating from $\delta r = 0$ cannot, regardless of their initial energy E, reach these curves and regions of phase space without a control mechanism.

7. Conclusion. In this paper several different tether models have been related mathematically, and it has been established in what limits they may provide useful models of tether dynamics. First, the massive tether model was linked to the slack-spring model through a conjecture on the limit of vanishing thickness. Then the slack-spring model was related to the billiard model in the limit of an inextensible tether. Next, the motion of the dumbbell model was identified within the dynamics of the billiard model through a theorem on the existence of invariant curves. Finally, numerical computations provided some insights into the dynamics of the billiard map for the case of an underlying circular orbiting center of mass.

The existence of the invariant curves within the planar billiard model with an underlying circular orbiting center of mass implies that the tethered system cannot reach these practically relevant, stable regions of phase space without control.

Acknowledgments. The authors thank Sergey Zelik, Jonathan Bevan, and David Lloyd for fruitful discussions.

REFERENCES

[1] R. A. Adams, *Sobolev Spaces*, 2nd ed., Academic Press, 1995.
[2] V. I. Arnol'd and A. Avez, *Ergodic Problems of Classical Mechanics*, 2nd ed., Mathematical Physics Monograph Series, W. A. Benjamin, ed., 1968.
[3] J. Ball, *Stability theory for an extensible beam*, J. Differential Equations, 14 (1973), pp. 399–418.
[4] V. V. Beletsky and E. M. Levin, *Dynamics of Space Tether Systems*, American Astronautical Society Publications 83, 1993.
[5] V. V. Beletsky and E. M. Levin, *Dynamics of the orbital cable system*, Acta Astronautica, 12 (1985), pp. 285–291.
[6] V. V. Beletsky and D. V. Pankova, *Connected bodies in the orbit as dynamic billiard*, Regular and Chaotic Dynamics, 1 (1996), pp. 87–103.
[7] J. Bellerose and D. J. Scheeres, *Energy and stability in the full two body problem*, Celestial Mechanics and Dynamical Astronomy, 100 (2008), pp. 63–91.
[8] N. Berglund and H. Kunz, *Integrability and ergodicity of classical billiards in magnetic field*, J. Statist. Phys., 83 (1996), pp. 81–126.
[9] M. P. Cartmell and D. J. McKenzie, *A review of space tether research*, Progress in Aerospace Sciences, 44 (2008), pp. 1–21.
[10] A. Celletti and V. Sidorenko, *Some properties of the dumbbell satellite attitude dynamics*, J. Celestial Mechanics and Dynamical Astronomy, 101 (2008), pp. 105–126.
[11] L. C. Evans, *Partial Differential Equations*, Graduate Studies in Mathematics 19, American Mathematical Society, 2000.
[12] R. W Farquhar, *Tether stabilization at a collinear libration point*, J. Astronautical Sciences, 49 (2001), pp. 91–106.
[13] G. Grubb, *Distributions and Operators*, Vol. 1, Graduate Texts in Mathematics, Springer Verlag, 2009.
[14] K. Uldall Kristiansen, P. Palmer, and M. Roberts, *Relative motion of satellites exploiting the super-integrability of Kepler's problem*, J. Celestial Mechanics and Dynamical Astronomy, 106 (2010), pp. 371–390.
[15] K. Uldall Kristiansen, P. Palmer, and M. Roberts, *Numerical modelling of elastic space tethers*, in preparation, 2011.
[16] M. Krupa, W. Poth, M. Schagerl, A. Steindl, H. Troger, and G. Wiedermann, *Modelling, dynamics and control of tethered satellite systems*, J. Nonlinear Dynamics, 43 (2006), pp. 73–96.
[17] M. Krupa, M. Schagerl, A. Steindl, P. Szmolyan, and H. Troger, *Relative equilibria of tethered satellite systems and their stability for very stiff tethers*, Dynamical Systems, 16 (2001), pp. 253–278.
[18] M. Krupa, M. Schagerl, A. Steindl, and H. Troger, *Stability of relative equilibria: Part* I: *Comparison of four methods*, Meccanica, 35 (2001), pp. 325–351.

[19] M. Krupa, M. Schagerl, A. Steindl, and H. Troger, *Stability of relative equilibria: Part* II: *Dumbbell satellites*, Meccanica, 35 (2001), pp. 353–371.
[20] A. Kuhn, W. Steiner, J. Zemann, D. Dinevski, and H. Troger, *A comparison of various mathematical formulations and numerical solution methods for the large amplitude oscillations of a string pendulum*, Appl. Math. Comput., 67 (1995), pp. 227–264.
[21] M. Leok, T. Lee, and N. H. McClamrock, *Dynamics of a* 3*D elastic string pendulum*, Proc. IEEE Conf. on Decision and Control, (2009).
[22] J.-L. Lions and E. Magenes, *Problémes aux Limites non Homogones*, 2nd ed., Vol. 2, Springer-Verlag, 1968.
[23] J. E. Marsden, *Lectures on mechanics*, London Mathematical Society, Lecture Note Series 174, Cambridge University Press, 1992.
[24] J. Moser, *Stable and random motions in dynamical systems*, Ann. Math. Studies, Princeton University Press, 1973.
[25] M. Pedersen, *Functional analysis in applied mathematics and engineering*, Vol. 1, Studies in Advanced Mathematics, Chapman & Hall/CRC Press, 1999.
[26] J. Peláez and D. J. Scheeres, *On the control of a permanent tethered observatory at Jupiter*, Paper AAS07-369 of the 2007 AAS/AIAA Astrodynamics Specialist Conference, Mackinac Island, Michigan, 2007.
[27] A. D. Polyanin, *Handbook of Linear Partial Differential Equations for Engineers and Scientists*, Vol. 1, Chapman & Hall/CRC Press, 2002.
[28] A. Pressley, *Elementary differential geometry*, 1st ed., Undergraduate Mathematics Series, Springer-Verlag, 2001.
[29] M. Sanjurjo-Rivo, F. R. Lucas, and J. Peláez, *On the dynamics of a tethered system near the collinear libration points*, Paper AIAA 2008-7380 of the AIAA/AAS Astrodynamics Specialist Conference, Honolulu, Hawaii, (2008).
[30] W. Steiner, *Transient chaotic oscillations of a tethered satellite system*, Acta Mechanica, 127 (1996), pp. 155–163.
[31] R. Temam, *Infinite Dimensional Dynamical Systems in Physics and Mechanics*, 2nd ed., Springer-Verlag, New York, 1997.
[32] D. Turaev and S. Zelik, *Homoclinic bifurcations and dimension of attractors for damped nonlinear hyperbolic equations*, in Nonlinearity, 16 (2003), pp. 2163–2198.